Transient transport of polymer solution flow in porous media

Aizhan Zeinula, Bachelor in Petroleum Engineering

Submitted in fulfillment of the requirements

for the degree of Masters of Science

in Chemical Engineering

School of Engineering

Department of Chemical Engineering

Nazarbayev University

53 Kabanbay Batyr Avenue,

Astana, Kazakhstan, 010000

Supervisor: Athanasios Papathanasiou

Co-supervisor: Vasileios Inglezakis

13.12.2018

DECLARATION

I hereby, declare that this manuscript, entitled “Transient transport of polymer solution flow in porous media”, is the result of my own work except for quotations and citations which have been duly acknowledged.

I also declare that, to the best of my knowledge and belief, it has not been previously or concurrently submitted, in whole or in part, for any other degree or diploma at Nazarbayev University or any other national or international institution.

Name: Aizhan Zeinula

Date: 13.12.2018

Abstract

Kazakhstan takes 12th place in World oil production, however 52,7 % of produced oil comes from “mature” fields that are on the last production stages. Therefore, use of enhanced oil recovery methods becomes essential; one of these methods is polymer flooding, which involves injecting a polymer solution into the reservoir in order to displace trapped oil towards the wellbore. For successful injection of polymer solutions in a reservoir it is essential to study properly their behavior in porous media. This master thesis focuses on that topic, by describing and understanding two main factors that have a great impact on polymer transport, namely (i) the inaccessible pore volume (IPV) and (ii) polymer retention due to its adsorption on grain surfaces within the porous medium. In order to reach this goal experiments on core samples (plugs) were conducted, and effluent concentration profiles were obtained. Moreover, numerical modelling was implemented to characterize diffusion/adsorption of polymer molecules inside the porous core.

Besides characterization of the porosity of the core samples, experimental work was based on the idea of contrasting the effluent concentration curves for polymer solution flow with the effluent concentration curves of a tracer (sodium chloride) during core flooding tests. The effluent concentration of tracer was measured by an on-line resistivity apparatus, while the polymer’s concentration was

determined indirectly by on-line measurement of pressure drop in a long coil tube, which was set right on the exit of the core plug. The adsorption was calculated during polymer injection in saturated core sample and was manifested as a delay on polymer effluent profile compared to the effluent profile of the tracer. The IPV, on other hand, was determined during brine injection after polymer injection, and manifested as faster polymer exit compared to the tracer; this is attributed to the multi–scale porosity of the core material and large size of the polymeric molecules. Experimental effluent profiles were compared to computer simulations using an in-house developed computer code.

Our results demonstrate that adsorption of polymer molecules on grain surface averages 0.0006 g/g, and that 14.8 % of the core plug's pore volume is inaccessible to the polymer solution. Also, according to mercury porosimetry, 16 % of the total pore volume has smaller diameter than the size of the polymer molecule; this points to a multi-scale porous structure, which is expected to affect effluent response curves. The transport of polymer through the core was described by a multi-scale dynamic convection/diffusion model which was implemented in-house using MATLAB. The shapes of curves of the polymer and tracer effluent curve can be reproduced by considering the polymer to have a higher Peclet number and lower diffisivity, whereas the tracer species is considered to have a higher microscale diffusivity and

lower Peclet number. This results is consistent with the analysis of the polymer size relative to the multi – scale porosity of the system.

Acknowledgments

I would like to thank Professor Athanasios D. Papathanasiou for his guidance throughout this research and incredible support even when I stopped believing in this work. Also my co-supervisor Professor Inglezakis for his assistance in this work and specifically his help in the characterization of core samples using mercury porosimetry.

I would also like to thank Dr. Adam Dobri for his invaluable help with the modeling part. He has helped with writing the code for MATLAB software and always was ready to give advice and feedback.

I also want to express my gratitude to Scientific Research Institute “CaspiiMunaiGas” for supporting this project and providing with all necessary equipment for conducting the experimental work.

Table of content

List of Abbreviations &Symbols

β	Partition coefficient, defined as β= $(C_l)_{eq}/(C_b)_{eq}$
$(C_l)_{eq}$	concentration in the bulk liquid at equilib- rium, mol/l
$(C_b)_{eq}$	concentration in the intraparticle pore volume liquid at equilibrium, mol/l
e	bed voidage
EOR	enhanced oil recovery
ep	particle voidage
IPV	inaccessible pore volume
NaCl	sodium chloride
ODE	Ordinary differential equations
PV	pore volume
Q	flow rate, m^3/min
r	Radius,mm
V	Volume,m^3
W_{rock}	weight of rock, gr
ΔP	pressure drop, psi
ΔPV	incremental change in pore volume
μ	dynamic viscosity, cP
μ_o	oil phase viscosity, cP
μ_w	water phase viscosity, cP
ν	kinematic viscosity, mm^2/s
ρ	Density, kg/m^3
ρ_r	Resistivity, ohm
σ	Conductivity, mS/m
φ	Porosity, %
$\mathcal{B}_m$	Biot number, dimensionless defined as $B_m = k_e R/D_{eff}$
$\mathbf{k_e}$	external mass transfer coefficient, cm/s
R	bead radius, cm
$\mathbf{D_{eff}}$	effective intraparticle diffusivity, cm*/s
$\mathcal{D}_r$	dimensionless diffusivity defined as $D_r = D_{eff}/(R^2(F/V_t))$
F	Volumetric flowrate, 1/s
V_t	total reactor volume, 1
$\mathcal{P}_e$	Peclet number, dimensionless defined as $P_e=(uL/D_l)$
u	axial superficial fluid velocity in the reactor
L	Reactor lenght
D_l	axial dispersion coefficient, cm2/s
ϑ	Hagenbach correction factor
ϕ	Thiele Modulus, $\phi=(R/3)(k/D_{eff})^{0.5}$
k	First order reaction constant, cm/s

List of figures

List of tables

Chapter 1-Introduction

“In Kazakhstan, 52.7% of produced oil is represented by mature oilfields that have passed through the production "plateau" or are at the last stage of reservoir production*"(Bulekbai, 2013).*

*“*More than half of the oil fields in Kazakhstan are mature, they have already passed the peak of production and the level of production is low. Currently, the oil recovery factor is 30%, while in the world it reaches about 50% - it is necessary to increase it by at least 5-7%' - *Bakytzhan Sagintayev, first deputy prime minister of the Republic of Kazakhstan (Tumasheva, 2015).*

Also it is a fact that a third of Kazakhstan GDP is generated by revenues from the oil and gas industry (Statistics, 2014).

Considering this information, the importance of tertiary recovery or enhanced oil recovery (EOR) becomes evident, as it plays a key role in the development of the national petroleum industry.

There are many EOR techniques that can be applied and have been applied successfully. However taking into the account that average depth of oil reservoirs in Kazakhstan is in the range 500-2500 m (200-8000 ft) and oil viscosity may vary from 100 to 900 cP, polymer flooding (injection) according to the figure 1.1 (Anon., 2012) could be chosen as tertiary recovery method.

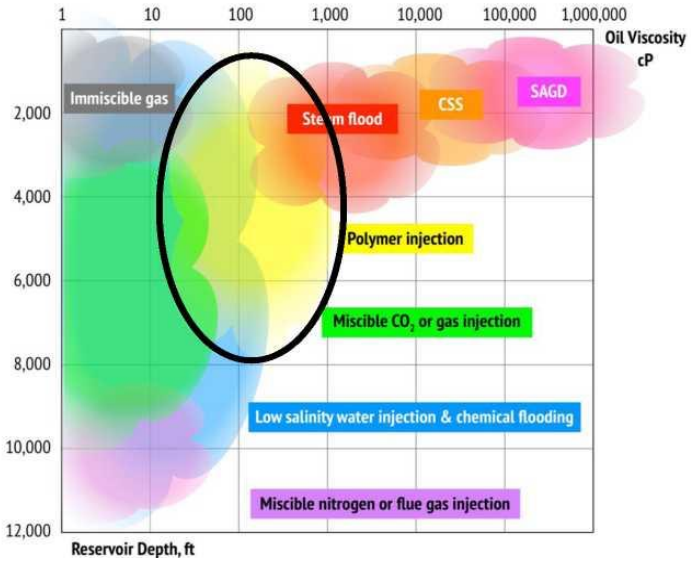

Figure 1.1 Regimes of application of tertiary oil recovery methods. The circled area and the yellow color outline the region (in terms of oil viscosity and reservoir depth) where polymer injection might be applied.

Larry W. Lake (Lake, 2010) gave a comprehensive definition of polymer flooding and how it works. Polymer flooding is a method in which a (water-soluble) polymer powder is added to the water that is injected in reservoir, making the resulting solution more viscous. As a result mobility ratio decreases, sweep efficiency increases and the remaining oil is displaced towards the wellbore. These terms will be explained in the following section.

Polymer flooding is the one the major category of chemical EOR methods which is designed to increase required mobility ratio between polymer and oil volume being displaced. However, the success or failure of polymer flooding is generally affected by reservoir geology, sweep efficiency, gravity segregation etc..

Unfortunately we cannot directly measure the majority of the variables needed for precise prediction of oil displacement during polymer flooding. A first step in improving this state of affairs is to understand the behavior of polymer solutions in a laboratory environment, specifically their flow behavior in porous core samples, obtained from the reservoir of interest. There are two main components that affect the polymer behavior in a porous medium, namely (i) polymer retention and (ii) inaccessible pore volume (IPV) (Idahosa, 2016). Polymer retention consist of mechanical entrapment, adsorption and hydrodynamic retention, while inaccessible pore volume refers to the inability of large polymer molecules to flow through small pore spaces. These parameters are determined through measurement of effluents' (polymer and tracer) profiles in one-dimensional core injection experiments. The data collected in such laboratory experiments are vital for further modelling of this EOR process (Ferreira et al, 2016).

In this study provides one-dimensional (1-D) core flooding experiments were performed, using polymer solution (hydrolyzed polyacrylamide) and tracers (sodium chloride), in order to better understand the transport behavior of the polymer molecules.

Chapter 1-Polymer flooding.

2.1 The concept of polymer flooding

The main function of injecting a polymer solution into oil reservoirs is to reduce the mobility ratio (defined by equation 1) of the displacing agent and oil, as well as an effective method of leveling the heterogeneity of the porous medium. The improved efficiency of flooding is achieved by adding a high molecular weight polymer which is dissolved in water. Even at low concentrations, addition of polymeric molecules significantly increases the viscosity of water and as a result it reduces its mobility and thereby increase the coverage of the layers. Figure 2.1 shows a schematic of polymer flooding (Lake, 1989).

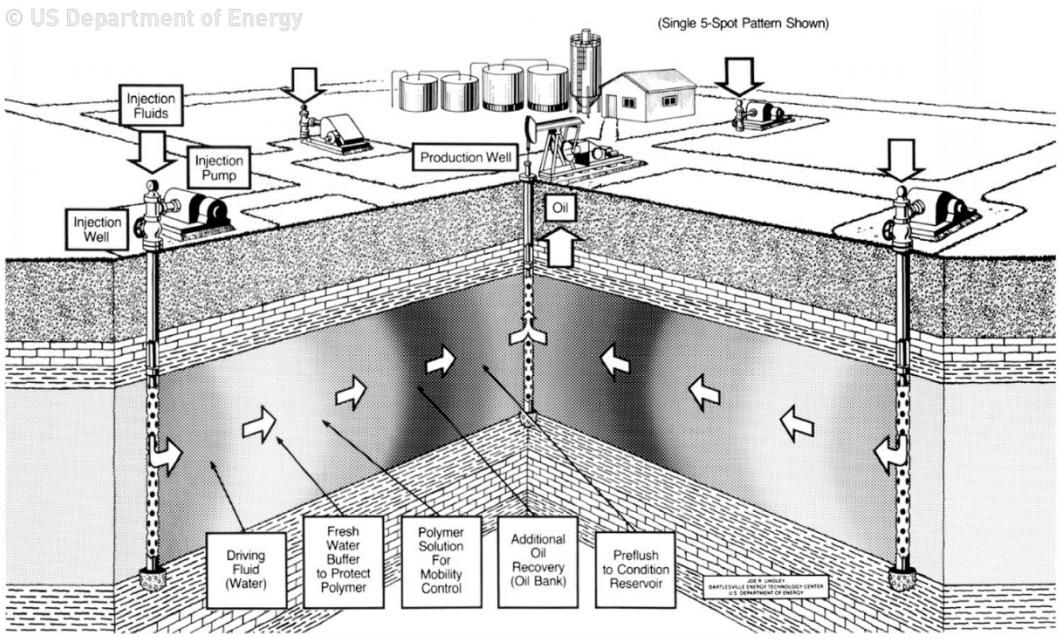

Figure 2.1 Process of polymer flooding (Lake, 1989)

In case where the viscosity of oil considerably exceeds the viscosity of the forcing-out agent (water) it is necessary to increase the viscosity of the pumped water and reduce its mobility; a direct consequence of this is that the minimum amount of water is used and also, that the maximum quantity of oil is recovered. Use of excess water leads to a significant reduction in final oil recovery (water uselessly circulates through the washed zones, and the oil stays in reservoir) and also to large economic losses associated with water pumping, recycling and transportation.

The Mobility Ratio (M) is determined as the ratio of the mobility of the injectant fluid (water or polymer solution) to the mobility of the displaced fluid (oil). The mobility ratio is a dimensionless number and an indicator of efficiency of displacemant:

$$M = \frac{\lambda_w}{\lambda_o} = \frac{k_w/\mu_w}{k_o/\mu_o}, \quad (1.1)$$

Where

λ_w- water mobility, mD/cP;

λ_0-oil mobility, mD/cP;

k_w, k_0- relative permeability of water and oil respectively, mD;

μ_w, μ_o- viscosity of water and oil respectively, cP;

For successful oil displacement, the Mobility Ratio (M) has to be less than 1. Otherwise, it was lead to viscous fingering effect i.e. water flows through washed zones, oil remains in the reservoir, and this will result in excess water production (watercut) (Don W. Green, 1998). One of the method to increase the mobility ratio is to adding chemicals in order to increase the water viscosity – thus the method of polymer flooding.

2.2 Worldwide experience and screening criteria for polymer flooding

The polymer flooding method in the world is studied since the end of the 1950s, and in industrial conditions is tested since the 1960s. Commercial experiments and also use of polymers in industrial volumes for the purpose of increasing oil production in various geological conditions were conducted on numerous locations worldwide: USA, Canada, China, France, India, Indonesia, Venezuela, Germany, Brazil, Argentina (Delamaide, 31 March-2 April 2014) . In recent years the world leader in the field of polymer flooding is China - projects on polymer flooding are implemented from the 1990s. Twenty-five years' successful experience of application of polymer flooding in China has shown that it can effectively be applied on fields with watercut higher than 95%, providing increase in oil recovery to 10% (Wang, 2008) (Chang, 2006) (Appendix A).

Polymer flooding is successfully applied on the large-scale Daqing oil field of China. This field is characterized by a complex geological structure and high heterogeneity of collectors. Reservoir oil average viscosity is 9 MPa.s, water is low-mineralized, and the reservoir temperature 113 °C. The PetroChina company since 1994 has carried out six pilot projects in layers with various collector (sandstone and conglomerate). The average increase in oil recovery in comparison with water flooding was 15 – 20% (Wang, 2008).

In Kazakhstan the first experience of polymer flooding was carried out on the field Kalamkas in 1981. This field's oil is heavy, highly-resinous, sulphurous, with viscosity up to 25 MPa.s in reservoir conditions. To prepare the polymer solution the Albian/Cenomanian water from specially drilled wells was a source for trial flooding. On the chemical composition Albian/Cenomanian water belongs to chlor-calcicitic type with the salinity 93 g/l, and density 1,07 g/cc. Originally in 1981 - 1983 the efficiency of polymer flooding was low due to high salinity and composition of the injected waters. In 1983-1986 in this field injection of viscoelastic structures has led to decrease in watercut from 1,5% to 0,2% a month. By 1990 the oil recovery was 33% at water content of 56%. At usual flooding such oil recovery can be reached at 98% watercut (98% of produced fluid is water) (Киинов, 1994) (Надиров Н. К., 1982).

The analysis of worldwide experience of this technology shows that polymer flooding can be conducted in fields with wide variety of geological properties. (Appendix A). Polymer flooding was used in the fields layered by

sands, sandstones and conglomerates, including clay sandstones. Successful application of polymer flooding has also been reported in limestone reservoirs, however, at the same time big losses of polymer due to adsorption are observed. Therefore the collector type in principle isn't the limited factor however from the economic reasons the terrigenous type of a collector is more favorable.

The fields' depth fluctuates within 579-2205 m. This parameter isn't limiting, however polymer flooding isn't recommended to be used in layers located as at very high and very low depths. In the layers located at a low depth, limiting factor is the injecting pressure which can approach the hydraulic fracturing pressure. In layers located at a higher depth the method is not recommended mainly because of high reservoir temperatures and the salinity of waters (Lake, 1989) (Taber, 1997).

The effective thickness of layers varies between 3-38 m, and average porosity in the range of 7-32%, in this regard these parameters aren't defining. One of the most important parameter is the average permeability of reservoir and its variability. When injecting solution of polymer in reservoirs with low permeability two problems can arrise: a decrease in well production and an increase in degradation of polymer solution due to high injection pressure. The lower limit of permeability is defined around 200 mD. In layers with high permeability increased concentration of polymer are required and this affects the economics of the process (Abou-Kassem, 1999) (J.J. Taber, August 1997).

The reservoir temperature should be varied from 33 to 77 ° C. At higher temperatures, thermal degradation of polymer can occur.

Analyzing the data presented in Appendix A (worldwide experience of polymer floodimg), it is obvious that desirable to use low-mineralized water to prepare the polymer solution, and where the reservoirs have highly mineralized water, fresh water buffer need to be injected to protect the polymer solution. For the first time this approach was implemented at the North Burbank field in 1970 (P.D. Moffitt, 1993) (Joseph C. Trantham, 1982).

Analysis of world experience shows that the maximum efficiency from the use of polymer flooding technology gives an oil increase 5-10% (Lake, 1989).

2.3 The effect of Inaccessible Pore Volume (IPV) on polymer effluent profiles

The term "Inaccessible Pore Volume" (IPV) was originally introduced by R. Dawson and R.B. Lantz in 1972. They found that not all open pore spaces can contribute to polymer flow and that pore spaces inaccecible to polymer molecules are filled with water resulting in polymer concentration changes (Dawson & Lantz, 1972). They related this phenomena to the differing size of pore spaces, some of which are too small for polymer’s molecule to flow through them. Therefore the term IPV is associated with the velocity enhancement of polymer solution comparing to tracer, as polymer’s molecule avoid small pore spaces and only flow through the macro-scale pores. In the experiments that were conducted by K.S. Sorbie (K.S. Sorbie,1991) larger velocity enhancement were observed for larger polymer's molecular size and in the cores with low permeability; IPV factor

do not depend from concentration or flow rate. However this statement a quite controversial, as Gupta and Trushenski (Gupta, 1978) reported that with some change in the concentration, velocity enhancement changes too, but later Lotsch (Lotsch, et al., 1985) did not noticed such change in his study. Stavland (Stavland, 2010)presented the following equation to calculate IPV:

$$IPV = 1 - \sqrt{\frac{1}{1+B}}, \tag{2.1}$$

where B is a dimensionless constant, calculated as k_W/k_P (ratio of water to oil permeabilities of the core sample)

However all the sources related to inaccessible pore volume underline that the inaccessible pore volume takes place when there is no adsorption (discussed later).

On the effluent profile, the presence of Inaccessible Pore Volume is demonstrated as followes (Dawson & Lantz, 1972):

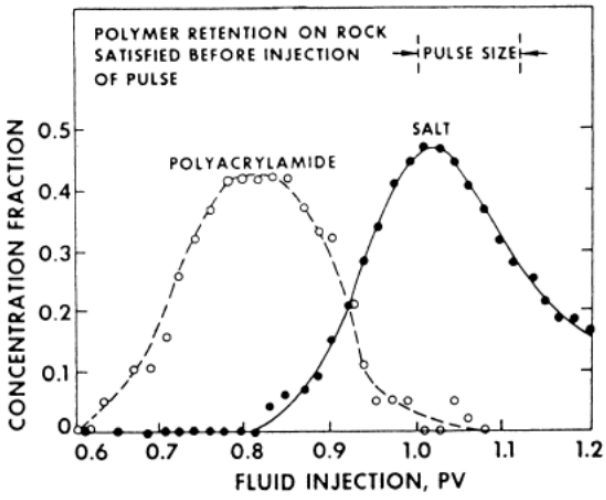

Figure 2.2 Original experimental demonstration of the inaccessible pore volume phenomenon (concentration fraction vs volume of injected fluid/pore volume of sample)

In the figure 2.2 is seen that the polymer flows faster than the tracer in a porous medium. Polymer is just too large to fit the small pore sizes therefore polymer just flow over it instead of flowing through pores. The tracer here helps to identify the inaccessible pore volume effect. Pancharoen, et al. concludes in his study that interpretation of IPVis best achieved with effluent profile comparing to the breakthrough curve (Pancharoen, et al., 2010).

2.4 The effect of retention on polymer effluent profiles

Retention has a great impact to the polymer flow in porous media as it includes to the adsorption, mechanical entrapment and hydrodynamic retention (Ferreira et al, 2016). Adsorption has the biggest effect on retention, which is considered an irreversible process. According to the D.G. Hatzignatiou, U. L. Norris and A. Stavland polymer retention is primarily caused by its adsorption on rock surfaces (Hatzignatiou, et al., 2013). D. Wang recommends choosing the size and molecular weight of polymer to be small enough in order for it to easily flow through porous media without clogging the pore space and mechanical trapping (Wang, et al., 2008). Moving to the mechanical entrapment and hydrodynamic retention, they are considered as reversible processes, controlled by changing the flow condition (Ferreira et al, 2016). A good way of illustrating this phenomena was found in the research of (Aluhwal, 2008) (figure2.3)

According to Sorbie & Phill the hydrodynamic retention is the least well studied mechanism of polymer retention, also there is the lack of comprehensive definition that will explain this process. (Sorbie & Phill, 1991). However Zhang

& Seright fully described this mechanism in their experimental study. They explained this kind of retention as a retention occurring due to hydrodynamic forces (Zhang & Seright, 2015). According to their laboratory data, it was proven that the hydrodynamic retention is directly affected by flow rate. Moreover, almost all hydrodynamic retention was irreversible, what is confirmed by unchangeable residual resistance factor (ratio of water mobility before and after polymer injection). However this study concluded that the enhanced oil recovery rheology is dominated more by intrinsic property (intrinsic viscosity, molecular eight and polymer's molecule size) than by retention. So they contradict the proposal of Chauveteau that rheology is primary related to retention (Chauveteau, et al., 2002).

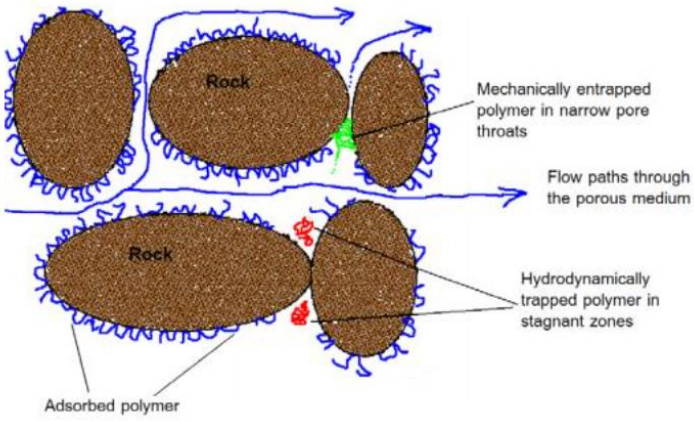

Figure 2.3 Polymer retention mechanisms in porous medium

Adsorption on other hand is physically present in porous media, and could dramatically decrease rock's permeability (Seright, et al., 2010). In the laboratory experiments on core flooding this phenomenon is manifested as a dramatic

increase in the pressure gradient when core is post-flushed with water in contrast to the water preflush. On the effluent profile adsorption is shown as delay comparing to the no adsorption (figure 2.4). Here is assumed the Langmuir form of the adsorption

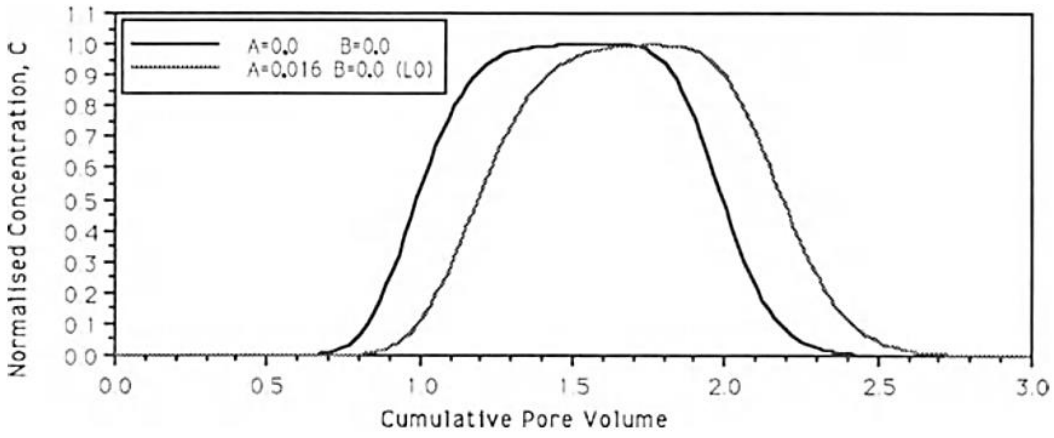

Figure 2.4 Calculated effluent profiles for a linear core system both with and without adsorption (L(0) - linear adsorption)

Chapter 3 - Methods and process of analyses.

3.1 Literature review of measuring methods of IPV and adsorption

There does not exist experimental apparatus or certain methodology to determine these parameters. However, K.S. Sorbie in his book stated that these two parameters can be calculated by constructing effluent profile concentration versus time (pore volume) and then contrasting the tracer and polymer effluenet profiles (K. S. Sorbie, 1991). Also, Lötsch et al. described in their paper that adsorption and IPV can be calculated by using tracers. A tracer needs to be added to the polymer solution in order to get polymer and tracer effluent curve (T. Lötsch, 1985). Almost all research methods of finding these two parameters by core flooding experiments are the same, the basic idea is contrasting tracer and polymer flow to get effluent profile. Adsorption can be determined by the delay of polymer that can be seen in difference between tracer and polymer curve. IPV, in its turn, can be measured by displacing polymer and tracer solution from the core with brine water. The polymer will be displaced quicker than the tracer, also tracer will be displaced from all pores, while polymer will be only displaced from the pores where it can flow. The number of pores which polymer can enter equals the entire pore volume minus the inaccessible pore volume (IPV).

3.1.1. Research methods of investigation inaccessible pore volume (IPV)

The first researcher who has reported the IPV term was Dawson and Lantz in 1977. They defined the inaccessible pore volume as the space which polymer's molecules hop, so the molecules of polymer are too large to fit in the pore space. (Dawson & Lantz, 1972) After they published their paper, many researchers have confirmed that by comparing polymer and tracer flow, concluding that polymer flows through porous media faster than tracer, when there is no adsorption due to inaccessible pore volume for polymer. (Dawson & Lantz, 1972; G. Paul Willhite, 1977; Chauveteau, 1982).

Stavland in his laboratory experiments measured IPV based on the difference between water and polymer solution permeability. So, the polymer solution was injected at different flow rates and the apparent viscosity was measured by stabilized pressure drop. He concluded that the apparent viscosity was less than the bulk viscosity at low shear rates, and this could be explained by the assumption that at low shear rates polymer does not enter the entire pore volume. Even though the IPV can be calculated, there is no methods to estimate the adsorption. (A. Stavland, 2010).

M. Pancharoen conducted experiment that proved that statement. To measure the IPV during core flood, the adsorption, first, was minimized by saturating the core with the 2000 ppm polymer solution until it reached equilibrium. Then the polymer was mixed with inorganic salt – NaCl and injected to core, after that the effluent was collected and separated into salt and polymer in order to measure

their concentration. The polymer concentration was determined by using a Ultraviolet–visible spectrophotometer (Lambda 35, Perkin-Elmer), while the concentration of salt were identified by titration with silver nitrate (AgNO3). Finally, to calculate IPV the difference between breakthrough curve of polymer and salt was used. And it was clearly seen from the experiment that polymer flows faster through core material if there is no adoption or it is minimized (M. Pancharoen, 2010).

3.1.2 Research methods of investigation polymer retention

C. Huh (C. Huh, 1990) used sodium bromide as a tracer to investigate polymer retention in porous media. The polymer solution with tracer was injected in a core plug with residual oil saturation at a constant rate until the effluent concentration stabilized. Then, polymer injection was followed by water injection to estimate the irreversible retention of the polymer from a mass balance. Effluent samples were collected and analyzed to measure polymer concentration by an HPLC method with a refractive index detector and concentration of tracer using ion chromatography. The work concludes that polymer retention increases with increase in polymer concentration and flow velocity.

D. Broseta in his laboratory measurements of polymer retention used potassium iodide (KI) as a tracer. He conducted the core flooding experiments under residual oil saturation conditions and 100% brine saturated core without any oil, also he tested the adsorption in hydrophilic and hydrophobic rocks. The adsorption/retention was calculated by the delay of polymer in effluent profile

(concentration vs pore volume) The concentration of the tracer was detected by UV spectroscopy, while the concentration of the polymer was measured using the Dohrmann carbon analyzer. Also, it was concluded that hydrophobic cores have stronger adsorption than hydrophilic, but in oil residual conditions the adsorption increases in hydrophilic cores due to additional adsorbing oil surface. (Daniel Broseta, 1995) The same tracer was used by R.N. Manichand in 2014. An in-line spectrophotometer, with wavelength detection 230 nm was used to detect tracer – KI and also polymer. However, unlike the previous experiment, the polymer concentration was calculated by the polymer viscosity that was measured using a small-diameter capillary tube that was set up on the exit of core holder with accurate digital pressure transducer. (R.N. Manichand, 2014). Using the pressure drop across the capillary tube, length and diameter of the tube and recording the time that polymer is needed to flow through the tube, viscosity was calculated using Poiseuille's equation (Womersley, 1955).

The classical tracer/polymer methods were conducted to measure polymer retention by J. E. Juri et al. However instead of using classical capillary viscometer, innovative inline viscometer was set at the effluent stream at anaerobic conditions. This allowed to avoid the problems of chemical degradation due to the reaction with oxygen. The effluent concentration was determined by COD (Chemical Oxygen Demand) and bleach method. They concluded that the extended injection and backflow test obtained accurate results on retention,

degradation, pressures and rates behaviors with no adjustable parameters (Juri, et al., 2015).

Unlike other researchers D.G. Hatzignatiou et.al experimentally investigated polymer flow in water and oil–wet core samples. Instead of using tracer in the polymer retention investigation, they connect capillary tube to core holder and measure pressure drop along the core holder and this capillary tube. Retained polymer volume was calculated based on the residual water saturation and the polymer breakthrough that is determined using plot of pressure drop across the core and the capillary tube. So, the injected polymer breakthrough occurs when the capillary pressure drop is equal to the average value of the pressure drop before and after breakthrough. Also, it needs to be noted that the average pressure is associated with a 50% concentration of a polymer solution. In their paper, they concluded that wettability has great impact on the polymer retention, indicating that oil-wet formation has the very low amount of retention comparing to the water–wet. This phenomenon is explained by the assumption that oil covers the boundaries of the rock grains, thus preventing polymer molecules to interact with them (Hatzignatiou, et al., 2013).

Wan investigated how oxygen presence impacts on polymer retention. In his paper, he measured the polymer retention by static (mixing with loose sand) and dynamic methods (core floods). Also, the experiments were conducted in conditions with presence of oxygen (aerobic), and with no atmospheric or dissolved oxygen (anaerobic). Potassium iodide (KI) was used as a tracer and

dissolved in polymer solution. It was underlined that from static retention measurements there is a little difference between aerobically or anaerobically conditions, while from the dynamic retention measurements there is too high polymer retention in aerobic condition which is explained by chemical degradation of polymer in presence of oxygen (Wan & Seright, 2016).

3.1.3 Research methods of investigation IPV and polymer retention

A detailed description about measuring of IPV and adsorption was given by Lötsch et al. In their research, they used inorganic salts as a tracer and to distinguish between the tracer and polymer they set up the densitometer and capillary viscometer in the exit (T. Lötsch, 1985). The adsorption has nonlinear relation to the concentration, when it is the reversible, so the adsorption could be described by a Langmuir or a Freundlich isotherm (Moore, 1963)

K.S. Sorbie, in other hand, used radioactive chlorine-36-beta - labelled brine. Polymer concentration were measured by a modified phenol-sulfuric acid method with an auto analyzer and the levels of beta radio- activity were determined with a Beckman TM scintillation counter. (K.S. Sorbie, 1987)

W.T. Osterloh and E.J. Law in their polymer transport experiments used salts as a tracer. They conducted four step injection experiment:

1. Injection of polymer and tracer until the effluent concentration is equal to the initial polymer concentration

2. Injection of brine until the effluent concentration of polymer and tracer is too low to measure

3. Repetition of step1

4. Repetition of step2

The polymer adsorption/retention was calculated by comparing the polymer effluent concentration in steps 1 and 3, the IPV was calculated by comparing the tracer and polymer effluent curves in step 3. The in-situ viscosity was calculated by measuring the pressure drop across core holder at various concentrations and rates. (Osterloh & Law, 1988)

E.S. Moe in his work investigate the IPV and polymer retention by ordinary tracer/polymer method. As a tracer was used inorganic salt, and the concentration of tracer was used based on its resistivity. The polymer concentration, on the other hand was calculated by measuring the viscosity of the polymer flowing through the coil that was set up on the exit of core holder. After constructing the effluent profile the IPV and retention was calculated by determining the area under effluent curves (Moe, 2015).

3.2 Procedures to measure IPV and adsorption

To meet master thesis objectives the methods of used in research Eline Moe (Moe, 2015) was chosen because the accurate concentration of tracer can be estimated through resistivity, based on the salt solution conductivity, and the

polymer concentration could be measured without contact with oxygen, so, the chemical degradation may be excluded .

The effluent profile is find by the following steps:

1. Prepare polymer solution with tracer in it
2. Inject the solution through core plug until pressure stabilization
3. Displace polymer solution with water until pressure stabilization

During the first injection of polymer solution with tracer (salt water) the tracer will come out first, and then the polymer solution, due to the adsorption of polymer solution on core's rock surface. During the second injection with water the polymer solution will be replaced faster than tracer due to inaccessible pore volume for polymer. The effluent curve is constructed based on the concentrations of the polymer solution and tracer and pore volume. Thus the adsorption is found by taking the integral between the tracer and polymer effluent curve during the injection of mixed solution through core plug. And the IPV is calculated by taking integral between polymer and tracer effluent curve during displacing with water.

The concentrations of the 2 curves (polymer and tracer) should be normalized to take the integrals by the following equation:

$$C_{norm} = \frac{C - C_{min}}{C_{max} - C_{min}}, \quad (3.1)$$

Where

C- concentration of fluid at the effluent

C_{min} - minimum concentration of fluid

C_{max} maximum concentration of fluid

The IPV is calculated by taking the integral over time (or number of pore volumes) of the difference between the normalized tracer concentration and normalized polymer concentration. The unit pore volumes, PV is the time divided by the amount of the time that it takes for one pore volume's worth of fluid to flow through the sample. The equation for IPV is

$$\text{IPV} = \int (C_{tr.norm} - C_{pol.norm})\text{dPV}\,, \tag{3.2}$$

where

$C_{tr.norm}$-normilized tracer concentration

$C_{pol.norm}$-normilized polymer concentration

PV- pore volume.

As the time – measurement (and therefore the number of pore volumes) is discrete, the integral is evaluated by the trapezoidal approximation.

The equation for the adsorption is

$$Adsorption = \{\sum[(C_{tr.norm} - C_{pol.norm}) * \Delta PV] + IPV\} * PV * C_{pol,max}/W_{\ rock,} \tag{3.3}$$

where

PV is the pore volume of the rock,

W_{rock} is the weight of the rock.

3.3 Polymer analysis

Analyses for 3 different polymers was conducted in order to choose one of them. The polymers were provided by the French company SNF. These polymers are used on the Kazakhstan's oil fields:

- FP 3630
- FP 5115
- FP 5205

3.3.1 Determination of the physicochemical properties of the polymer

The method is based on the calculation of the non-volatile content substances in powdered polymers by loss in weight after drying. The purpose of measuring this method is to determine polymer content in polymer powder to prepare solution with accurate concentration.

Equipment, reagents and materials:

- Weighing bottles;

- Analytical balance with weighing accuracy 0.0001 g;

- Desiccator

- Drying or heating cabinet (T = 105 ± 2 ° C).

Weighing bottles washed with chrome mixture, and after washed 2-3 times with distilled water. The washed weighing bottles are dried in a drying cabinet at 105 ± 2 ° C to a constant weight. Dried weighing bottles are stored in a desiccator.

A pre-dried to constant weight and weighted portion of the polymer is placed in the weighing bottles, then it is evenly distributed on the bottom of the weighing bottles. The weighing bottles is capped and weighed. The result is recorded in grams accurate to the fourth decimal place.

The open weighing bottles with the sample is placed in a drying cabinet and dried at a temperature of 105 ± 2 ° C to constant weight (weight change not more than 0.0005 g). After drying, the bottles are cooled in a desiccator to room temperature and weighed. The first weighing is carried out after 2 hours of drying, the next after 0.5 hours. The degree of rounding weighing results is 0.0001g.

The polymer content is calculated as a percentage using the equation:

$$W = \frac{m_1 - m_2}{m} 100\ \% \qquad (3.4)$$

Where

m_1 – mass of weighing bottles before drying, gr;

m_2 – mass of weighing bottles with polymer powder before drying, gr;

m – mass of polymer powder, gr;.

3.3.2 Determination of the polymer solution hydrolysis degree

The method is based on direct titration of the carboxyl groups of the acrylamide polymer in aqueous solution with alkali. There is a relation between molecular weight and hydrolysis degree, the higher the molecular weight the higher the hydrolysis degree. High molecular weight results in larger moleculas size (described later), and results in high IPV effect. However high hydrolysis results in low adsorbtion, as the negative carboxyl groups are repulces from negatively charged core samples' particle surface (F.D. Martin, 1975). Thus, the hydrolysis degree is one of the parameter to choose the optimum polymer solution that will be used in experimental work.

Equipment, reagents and materials:

- Analytical balance with weighing accuracy 0.0001 g;
- paddle stirrer for highly viscous media;
- Titration installation in accordance;
- Magnetic stirrer;
- pH meter with a measurement error of 0.05;
- Glass cylinder;
- Glass cup;
- Burettes;
- 0.1 molar solution of HCl;
- 0.05 molar solution of NaOH;
- Distilled water according.

For the analysis polymer solution with a concentration of 0.05-0.1% in distilled water is used. A portion of the polymer is calculated taking into account the mass fraction of the main substance by the equation:

$$m = \frac{C*P}{W}, \quad (3.5)$$

Where

C – polymer concentration in solution, %;

P – polymer solution mass, gr;

W – polymer content (activity of polymer solution), %.

The calculated mass of the polymer is weighed on an analytical balance with an accuracy of the third decimal place. Distilled water is poured into the beaker in the volume required for the analysis, minus the weight of the polymer sample. A glass of water is placed under the paddle stirrer and the stirring is turned on; the speed of mixing should ensure the creation of a funnel. The polymer is putted evenly among the funnel. The polymer solution is dissolved until complete homogenization, dissolution evaluation is carried out visually by the absence of polymer globules and solution uniformity. For analysis, the 200 cm3 of polymer solution is took, then pH is measured and up to value to pH = 3.8 with hydrochloric acid. Then titration is carried out with sodium hydroxide solution to pH 7.5. The volume of NaOH solution, used to titration of the polymer solution is measured. At the same time the control measurement with the same volume of

distilled water is performed with the same operations as with the working sample of the polymer. The degree of hydrolysis of the polymer in percent is calculated by the following equation:

$$\alpha = \frac{(V-V_o)*C*M*10^{-3}}{m-(V-V_o)*C*23*10^{-3}}, \quad (3.6)$$

where

V and Vo – volume of NaOH solution spent on working and blank sample titration, ml;

m – the weight of the polymer sample contained in the solution taken for titration, g;

C - exact molar concentration of the NaOH solution, mol / l;

M - molar mass of acrylamide, g / mol;

23 - molecular weight of sodium, g / mol;

10^{-3} - conversion factor from cm^3 to dm^3

As a result of the analysis is taken the arithmetic average of two parallel measurements, the difference between them should not exceed 0.5%. The results were rounded up to 0.1%.

If a polymer manufacturer provides a technical documentation with different methods for determining degree of hydrolysis, then whole analysis is performed in accordance with the manufacturer's documentation.

3.3.3 Measurement of the intrinsic viscosity for the calculation of the molecular weight and molecule diameter of the polymer

This method is based on measurement of time taken for a solution of dilute polymer and sodium chloride to flow through a capillary viscometer of a certain diameter. By measuring the intrinsic viscosity the molecular weight can be calculated, and by calculating the molecular weight diameter of polymer molecules can be identified. By knowing the molecules' size and pore size distribution, the rough assumption about fitting the polymer molecules in pore size may be done. The result is obtained by using the procedure for viscosity measurement of polymer solutions with different concentrations and by extrapolating the experimental data to zero concentration in accordance with the Huggins equation:

$$\eta = [\eta]+KC[\eta]^2 , \qquad (3.7)$$

where

η_{rv} - reduced viscosity, dL / g;

$[\eta]$ - intrinsic viscosity, dL / g;

C - polymer concentration, g / dL;

K - the Huggins constant.

Equipment, reagents and materials:

- Analytical balance with weighing accuracy of 0.0001 g;
- Blade mixer with adjustable rotation speed;

- Ubbelohde viscometer with a capillary diameter 0.54 or 0.84 mm;

- Mechanical stopwatch with 0.2 s. scale;

- Cylinder;

- Pipette 1.2-2-20 and pipette 1.2-2-5.10;

- Glass;

- Pear rubber;

- Thermostat suitable for glass viscometers, that maintains the temperature of 25 ± 0.1 ° C;

- Sodium chloride, pure and filtered solution with a mass fraction of 10%,;

- Distilled water according;

- Acetone;

- Chrome mix.

Before making measurements on the viscometer, a portion of a polymer with mass of 1.5-3.0 g. is weighed (the result is recorded in grams up to the fourth decimal place) and evenly added with stirring to a solution of sodium chloride with a volume of 100 cm^3. The mixture is stirred in a blade mixer until the solution is completely homogenized. In addition, dissolution rate should be visually checked every 15 minutes by pouring the solution from one glass to another.

The mass concentration (C) of the obtained polymer solution is calculated by the equation:

$$C = \frac{m*W}{V*100}, \quad (3.8)$$

where

m - the mass of the polymer sample, g;

W - the mass fraction of the main substance in the polymer,%;

V - the volume of sodium chloride taken to dissolve the polymer, dL.

Before taking measurements, the viscometer is washed with a chromium mixture, rinsed with distilled water, acetone, and dried. 20 cm^3 of the filtered polymer solution is placed into the Ubbelohde viscometer by pipette, then whole viscometer is moved into thermostat for 10-15 minutes at a temperature of 25 ° C. At the same time, it is necessary to ensure that the capillary and the viscometer ball are completely immersed in a thermostatic liquid. The polymer solution is sucked into the viscometer ball just above the top mark by using a rubber bulb with a tube assembled on the knee of the viscometer. Furthermore, the second knee of the viscometer should be closed using clamp on a rubber tube assembled at the end of the knee. Then the clamp is slightly opened and at the moment when the polymer solution passes the upper mark, stopwatch starts tracking time for polymer solution to flow from the upper mark of the measuring ball to the lower mark. This test is carried out at least three times and then the average value of three parallel measurements is calculated. After that, the polymer solution is diluted in the viscometer itself by consistently adding 4.0 cm3 of sodium chloride solution thoroughly mixed with a pear. Then whole viscometer is thermostated again, and after each dilution time taken for polymer solution to drain is determined.

The mass concentration of dilute polymer solutions (C_i) is calculated by the equation:

$$C_i = \frac{m*V}{V_p}, \quad (3.9)$$

Where

C - the initial mass concentration of the polymer solution, g / dL;

V - initial volume of the polymer solution, cm^3;

V_p - volume of the diluted polymer solution, cm^3.

At least five dilutions should be made considering that the correct limiting viscosity number measurement, the solutions concentration in the viscometer should be limited to the area where the relative viscosity lies in the range 2.0 - 1.2. Sodium chloride solution used for dilution should be thermostatted in the same thermostat. By the end of the test, the viscometer should be accurately washed, dried, and then 20 cm^3 of sodium chloride solution is poured and the time for the solvent to drain is measured by the above method. Measurement and calculation data are entered in table 3.1.

Table 3.1Table for measuring intrinsic viscosity

Measurements	V_1	V_2	V_3	V_4	V_5
Polymer drainage time , sec. (t)	t_1	t_2	t_3	t_4	t_5
Solvent drainage time, sec. (t_0)	t_0	t_0	t_0	t_0	t_0
Relative viscosity $\eta_{rel}=t/ t_0$	η_{rel1}	η_{rel2}	η_{rel3}	η_{rel4}	η_{rel5}
Specific viscosity $\eta_{sp} = \eta_{rel} -1$	η_{sp1}	η_{sp2}	η_{sp3}	η_{sp4}	η_{sp5}
Mass concentration of polymer solution, g/dL C_i	C_1	C_2	C_3	C_4	C_5
Reduced viscosity, dL/g η_{sp}/ C_i	η_{sp1}/ C_1	η_{sp2}/ C_2	η_{sp3}/ C_3	η_{sp4}/ C_4	η_{sp5}/ C_5

Data is processed by graphical method concentration C versus reduced viscosity $\eta_{sp/}$ $C_{i.}$ Through the data points straight line is constructed until intersection with y-axis. The intersection point equals to the intrinsic viscosity.

To calculate the molecular weight the following following equation of is used (Flory, 1953):

$$[\eta]=K'*M^a\ , \qquad (3.10)$$

Where

M – is molecular weight

K', **a** are empirical constants for the system polymer – solvent

The diameter of polymer molecule in μm is found by the equation (Flory, 1953):

$$d_p=8(M*[\eta])^{1/3}\ , \qquad (3.11)$$

3.3.4 Polymer solution preparation

Considering the established concentration of polymer solution, calculation for determination of quantity of the dry polymer powder required for preparation the necessary amount of polymer solution is calculated by a equation:

$$W_{pr} = \frac{W_s*C_s*10^{-4}}{A_{pr}}, \qquad (3.12)$$

Where

W_{pr}- weight of dry polymer powder, g

W_s – weight of polymer solution, g

C_s – polymer solution concentration, ppm

A_{pr} – activity of polymer solution, % (90-95 %).

The amount of the necessary water required for preparation of necessary volume of polymer solution is determined by the equation (8).

$$W_{bs} = W_s - W_{pr}, \quad (3.13)$$

where:

W_{bs} – weight of water for preparing polymer solution, g.

After determination of necessary parameters (W_{pr}, W_{bs}), using the glass, the magnetic stirrer and water, polymer solution was prepared. The preparation time is approximately 2-3 hrs. The polymer solution with concentration 2000 ppm was prepared.

3.3.5 Rheological properties of polymer

Rheological characteristics of polymers was determined on the rheometer - Anton Paar MCR 502 at the room temperature and shear speeds from 1 to 100 with-1. Processing of results were conducted by software of RHEOPLUS/32 V3.62. By results of test dependences of dynamic viscosity on shear speed are constructed.

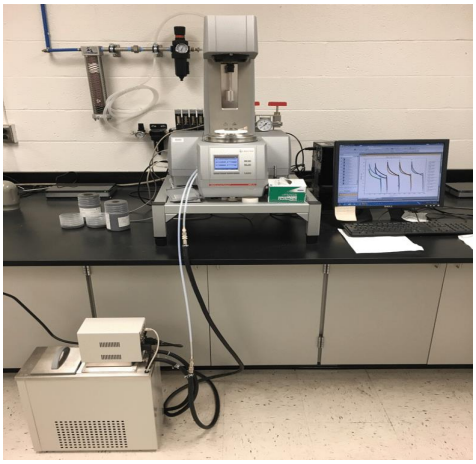

Figure 3.1 Rheometer - Anton Paar MCR 502

3.4 Core analyses

Core analyses on 6 different samples was conducted in order to choose one.

3.4.1 Core extraction

For core material analysis, determination of their various properties, it is necessary to have a pure sample of this rock, devoid of all fluids saturating it. In this regard, the ready samples after obtaining the correct shape of the cylinder and symbols have been sent for extraction.

The extraction means the process of sample pore space cleaning from oil, bitumen, water and salts. The samples extraction in our case was carried out on Soxhlet. Prior to extraction, the plugs have been weighed on an analytical balance with accuracy to 0.001 g.

Figure 3.2 Soxlet apparatus for core sample's extraction

The samples cleaning have been carried out Soxhlet apparatus with washing by organic solvents. As the solvent, the alcohol-benzol mixtures have been used. The principle of Soxhlet apparatus operation is very simple. The solvent vapors enter through a side tube in the extractor, and then in a refrigerator, are condensed and liquid thus formed fills the container, where the sample are, which are in the extractor. When the fluid in the extractor reaches the knee of the outlet tube (siphon), it flows back into the flask, and wherein the solvent boils.

During the cleaning process, the samples have been tested for luminescence under UV light. In conjunction with the solvent color, this procedure has been used to determine the indicator of cleaning from hydrocarbons (HC). After full cleaning, all samples at temperature of 1050C have been dried in the drying oven (DKN 600) to the constant weight.

3.4.2 Measurement of porosity, bulk and mineralogical density of rock samples with helium porosimeter

In order to measure the reservoir porosity and permeability, the computer station “Abacus” of automated data input by weight and size of the sample have been used. The results of samples weighing on an analytical balance with accuracy to 0.001g, and the average value of sample size determined by means of digital caliper ruler (length and diameter is measured up to 10 times) automatically have been filled in a specially created table.

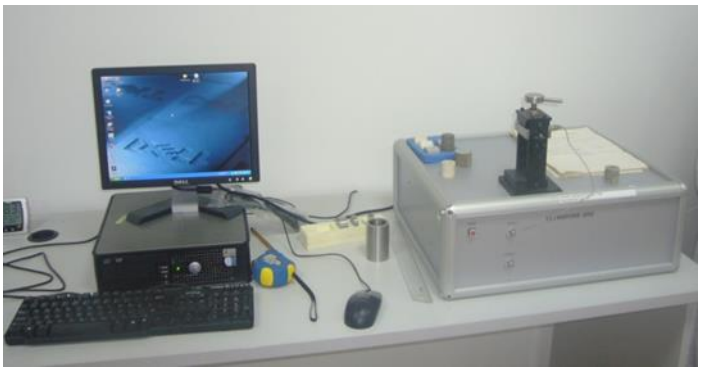

Figure 3.3 Ultrapore 300 - helium porosimeter

After obtaining the basic parameters of weight and volume, the samples have been placed in the glass desiccator in order to reduce the adsorption of atmospheric moisture and transferred to further conventional analysis (determination of porosity and gas permeability).

In order to measure the volume of samples grain the calibrated helium porosimeter (ULTRA-PORE 300) have been used operating on the principle of Boyle's Law (3.14).

$$P_1 \cdot V_1 = P_2 \cdot V_2, \tag{3.14}$$

The equation used to calculate the grains volume is derived from the basic equation of Boyle's law as follows:

$$P_1 \cdot V_{Ref} = P_2 \cdot \left(V_{Ref} + V_{\text{matrix}} - V_{\text{Grains}}\right), \tag{3.15}$$

where:

P_1 - pressure in comparison chamber;

V_{Ref} - volume of comparison chamber, cm^3;

P_2- pressure after helium diffusion in core glass;

V_{matrix}- volume of core glass, cm^3;

V_{grains}- volume of sample grain, cm^3.

Further porosity (3.16), bulk density (3.17) and mineralogical density (3.18) of rock sample have been calculated using the equation below:

$$\varphi = \frac{(L \cdot \pi \cdot \frac{D^2}{4}) - V_{\text{Grains}}}{(L \cdot \pi \cdot \frac{D^2}{4})} \cdot 100, \quad (3.16)$$

$$\rho_{\text{volume}} = \frac{m_{\text{sample}}}{(L \cdot \pi \cdot \frac{D^2}{4})}, \quad (3.17)$$

$$\rho_{\text{miner}} = \frac{m_{\text{sample}}}{V_{\text{Grains}}}, \quad (3.18)$$

where:

φ – sample porosity, %;

L– sample length, cm;

D – sample diameter, cm;

ρ_{volume} – bulk density of sample, g/cm^3;

ρ_{miner} – mineralogical density of sample (grain density), g/cm^3;

m_{sample} – dry weight of sample, gr.

It should be noted that determined porosity is meant as open porosity and accordingly, the mineralogical density of rock has an apparent mineralogical density, if closed porosity is present in the analyzed sample. Bulk density is the ratio of mass of core plug to the bulk volume, while grain density is the density of rock - forming minerals.

3.4.3 Measurement of samples permeability on nitrogen permeameter

Measurement of the absolute permeability of samples has been carried out using gas (nitrogen) on the calibrated equipment ULTRA-PERM 600 equipped with new mass flow meters and pressure sensors. The software makes the calculations using Darcy and Klinkenberg equations to calculate the gas permeability and reciprocal of average pressure.

Figure 3.1 ULTRA-PERM 600 - Nitrogen permeameter

The Darcy equation as applied to compressible gasses is used by the software to calculate the gas permeability. This has the following form:

$$K_g = \frac{1000 \cdot P_1 \cdot \mu \cdot Q_1 \cdot L}{(P_1^2 - P_2^2) \cdot A}, \tag{3.19}$$

where:

Kg – gas permeability, mD;

μ– gas viscosity, cP;

Q_1 - gas flow value, cm^3\sec;

P_1– input pressure, atm;

P_2– downward pressure, atm;

A– section area of sample perpendicular, cm^2;

L– sample length, cm.

3.4.4 Measuring pore size distribution using mercury porosimetry

In this method, at each pressure step the saturation of pore space with mercury is estimated by determining the amount of mercury remaining in the penetrometer tube. As the pressure increases, mercury penetrates into the pore structure from the tube. The volume of mercury in the penetrometer is measured by determining the electrical capacity of the penetrometer. Mercury porosimetry (POREMASTER 60) is based on the capillary principle, which causes the penetration of liquid into small pores. This principle is expressed by Young-Laplace equation (3.20):

$$P_c = \sigma\left(\frac{1}{R_1} + \frac{1}{R_2}\right), \tag{3.20}$$

where

P_c – capillary pressure, kPa;

σ – surface tension, kPa/cm;

R – radii of curvature, cm

For cylindrical porous tube model, the two radiuses of curvatures are similar, and the Young-Laplace equation (3.20) becomes:

$$P_c = \frac{2\sigma}{R}, \tag{3.21}$$

The relationship between the radius of curvature and the radius of a capillary tube is:

$$\cos\theta = \frac{r}{R} \rightarrow \quad \frac{1}{R} = \frac{\cos\theta}{r}, \tag{3.22}$$

By replacing (3.22) for (3.21), Young-Laplace equation for cylindrical porous tube model:

$$P_к = \frac{2\sigma \cdot \cos\theta}{r}, \tag{3.23}$$

where

P_c – capillary pressure, kPa;

σ – surface tension, kPa/cm;

θ – contact angle, °;

R – radius of curvature, cm

The capillary pressure is related to the mercury injection pressure:

$$P_c = P_{mercury} - P_{air}, \tag{3.24}$$

Since the test starts with a vacuum, $P_{air} \approx 0$, equation (3.25) will be:

$$P_c = P_{mercury} = \frac{2\sigma_{mercury-air} * cos\theta}{r_i}, \tag{3.25}$$

By solving equation (3.25) for r_i, the pore size:

$$r_{P_{mercury}} = \frac{2\sigma \cdot \cos\theta}{P_{pmymu}}, \tag{3.26}$$

where,

r_i – pore radius in sample, mkm;

σ – surface tension between mercury and air, kPa/cc;

θ – contact angle, °;

$P_{mercury}$ –mercury injenction pressure, MPa.

The effect of surface tension between mercury and air is expressed through the contact angle:

$$r_i = 0{,}145038 \cdot \frac{2 \cdot 485 \cdot \cos 130}{P_{pn}\ P_{mercur}} = \frac{90{,}43161}{P_{pmy}\ P_{mercur}} \qquad (3.27)$$

The total volume of mercury in the penetrometer at the transition from the low-pressure to the high-pressure is given by the equation:

$$V_{mercury} = \frac{\Delta w}{\rho_{mercury}}, \qquad (3.28)$$

Where

Δw – difference in the weight of sample,

$\rho_{mercury}$ – density of mercury, g/cc.

The total amount of mercury in the penetrometer is expressed by the following:

$$V_{mercury} = V_{pen} - V_s \ \rightarrow \ V_s = V_{pen} - V_{mercury}\ , \qquad (3.29)$$

where,

V_{pen} – volume of penetrometer, ml;

$V_{mercury}$ –volume of mercury in penetrometer measured before going from the low-pressure to the high-pressure, ml.

V_s – total volume of sample, ml.

The following conversion values were applied for calculations:

Parameter	System			
	«gas-mercury»	«gas-reservoir brine»	«gas-oil»	«oil-reservoir brine»
Mercury contact angle	130			
Mercury IFT	485			
Labouratory contact angle		0	0	30
Labouratory IFT		70	24	35
Contact angle of the collector		0		30
IFT of the collector		50		25
Labouratory TcosTheta		70	24	30,3
Collector TcosTheta		50		21,7

IFT – Inverse Fourier Transformation, IFT * cosin of contact angle: 311,8

The results of 6 samples are presented in **Appendix B**

Chapter 4 Main experiment

4.1 System for experiment

For carrying out tracer experiments on core plugs, the PLS-200 system (figure 4.1) with 4 hydrostatic coreholders was used. Samples were initially saturated with salt water – 100 g/l NaCl, and then plugs were inserted in hydrostatic coreholders.

Figure 4.1 PlS-200

For sample saturation with salt water, an automatic saturator (AST-600) (Figure 4.2) was used, which allows to choose in the automated order time of pumping of air and pressure of saturation for fast and full saturation of samples of a core.

For water and polymer injection two-cylinder piston pumps and cylindrical container with piston replacement were used, so the accurate flow rate may be controlled.

At the effluent of the core holder steel coil with length 4.14 m and diameter 0.89 mm was established, the pressure gradient inside the coil was measured in order to calculate the concentration of polymer solution at the effluent.

After the coil to measure resistance of the effluent Fluke apparatus (figure 4.3) was set in order to calculate the concentration of the tracer. A diagram of the core flooding experimental set up is shown on the Figure 4.4.

Figure 4.2 AST-600 Autosaturator for sample saturation

Figure 4.3 Fluke Fluke PM 6306 for resistance measurement of effluent

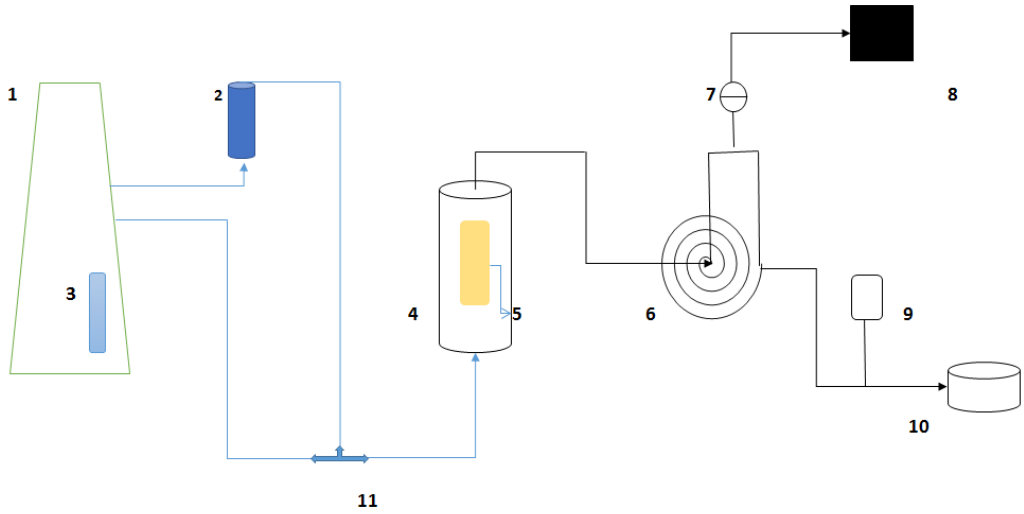

Figure 4.4 Scheme of the system used in experiments

1) Pump
2) Flask with polymer solution and tracer (150 g/l NaCl)
3) Cylindrical container with salt water (100 g/l NaCl)
4) Core holder
5) Core plugs
6) Steel coil
7) Pressure transducer
8) PC
9) Fluke resistance apparatus
10) Flask
11) Three – way valve

The procedures of conducting experiment:

1. 100% saturated with 100 g/l NaCl core plug were inserted in core holders and closed hermetically

2. Polymer solution with tracer (150 g/l NaCl) in cylindrical container -3 were pumped form down to core holder with flow rate 2 ml/min
3. The effluent goes through the coil first, pressure gradient measured and sent to computer
4. After the coil the effluent goes through resistance apparatus, the data were collected via wed-camera
5. After pressure and resistance stabilization the pump was switched to the salt water (100 g/l NaCl) in order to find IPV.
6. The step 4 and 5 repeated.

4.2 Data processing.

4.2.1 Construction of the polymer vs. concentration curve

To construct polymer curve concentration versus time, pressure gradient in coil was recalculated to the viscosity by the using Hagen-Poiseuille equation:

$$\mu = \frac{\Delta P \pi r^4}{8LQ}, \tag{4.1}$$

where

ΔP- pressure gradient through coil

r-radus of the coil tube (0.445 mm)

L – length of the coil tube (4.14 m)

Q- flow rate of liquids. (2 ml/min)

To find the concentration of polymer through measurement of viscosity during the experiment the relationship between concentration and viscosity must be determined. For this purpose the viscosity of polymer solutions at different concentrations was measured with capillary viscometer. (Figure 4.5)

The polymer solution is filled in tube 2 until it reaches the line 8. Then the time of flowing solution between mark 5 and mark 7 is recorded. These steps repeated 3 times for accurate result.

Knowing the calibration constant for each viscometer (K) the kinematic viscosity is found by equation (4.2)

$$v=K*(t-\vartheta), \qquad (4.2)$$

Where

t- time, sec

ϑ - the Hagenbach correction factor. $\vartheta = 0$ when t < 400 sec

The dynamic viscosity is calculated by equation 4.3.

$$\mu = \rho * v, \qquad (4.3)$$

The relationship between polymer solution concentration and viscosity is shown on the figure 4.6

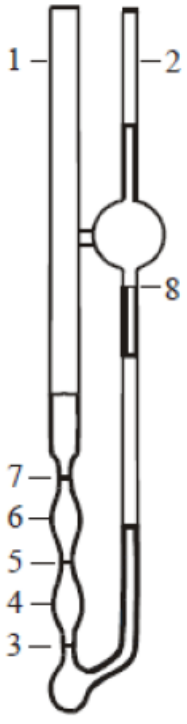

Figure 4.5 Capillary type viscometer

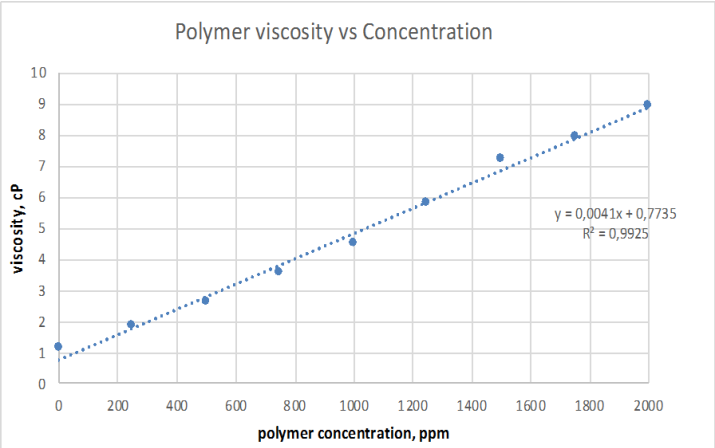

Figure 4.6 The relationship between polymer solution concentration and viscosity

The relationship can be expressed by equation 4.4

$$y = 0.0041x + 0.7735, \quad (4.4)$$

So the polymer concentration is found by equation 4.5

$$C_{pol} = (\mu - 0.7735)/0.0041, \quad (4.5)$$

4.2.2 Construction of the tracer concentration vs. conductivity curve

Tracer curve was constructed based on the relationship between salt water conductivity and concentration. The core was initially saturated with 100 g/l NaCl, while the tracer concentration was 150 g/l NaCl, and the concentration of displaced water was 100 g/l NaCl.

The conductivity (σ) of water was calculated through the measured resistivity (ρ)

$$\sigma = 1/\rho, \quad (4.6)$$

The relationship between tracer salinity (concentration) and conductivity is shown on the figure 4.7.

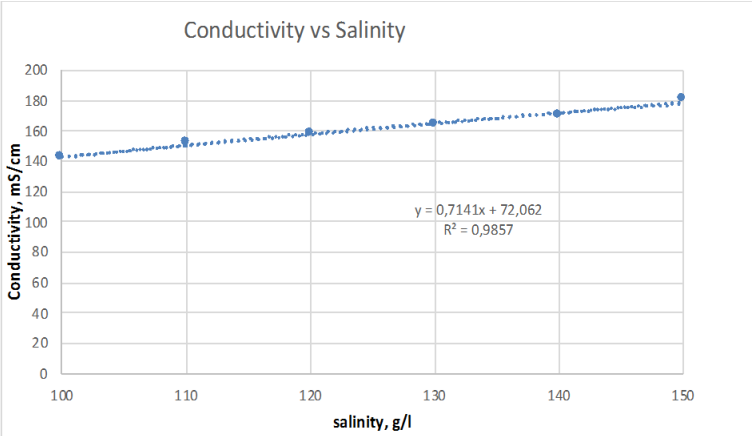

Figure 4.7 The relationship between tracer salinity (concentration) and conductivity

Thus, the tracer concentration can be calculated by the equation 4.7.

$$C_t=(\sigma\text{-}72.062)/0.7141, \qquad (4.7)$$

Chapter 5 – Results and discussions of experimental analyses

5.1 Results of polymer solutions analyses

Three polymer powder was analized before conducting experimental work. The polymer content, hydrolysis degree, molecular weight, diameter of polymer molecules and rheological properties was identified. The raw data and calculated values are presented in Appendix C.

Table 5.1 The physicochemical properties of polymer solution

	Polymer content (activity of polymer solution), %	Hydrolysis degree, %	Intrinsic viscosity, dl/g	Molecular weight, g/mol *10^6	Diameter of polymer molecule, μm
FP 3630	90.27	25	19.452	10.07	0.474
FP 5205	90.36	15	17.613	9.90	0.447
FP 5115	90.6	11	16.790	9.61	0.435

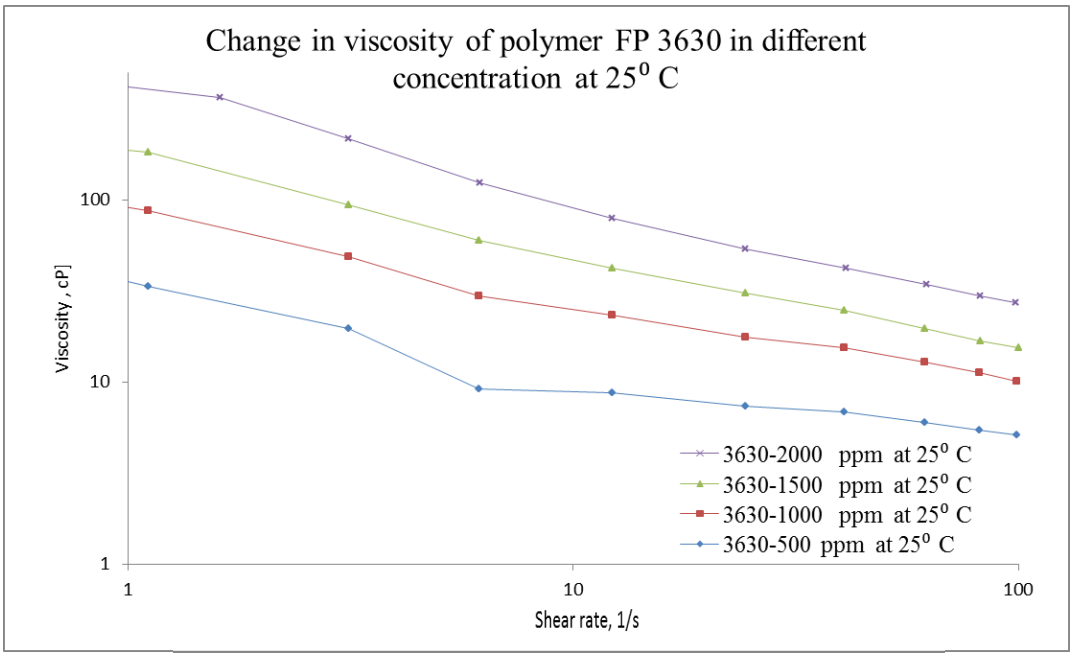

Figure 5.1 Rheological data of polymer FP3630 (log-log chart)

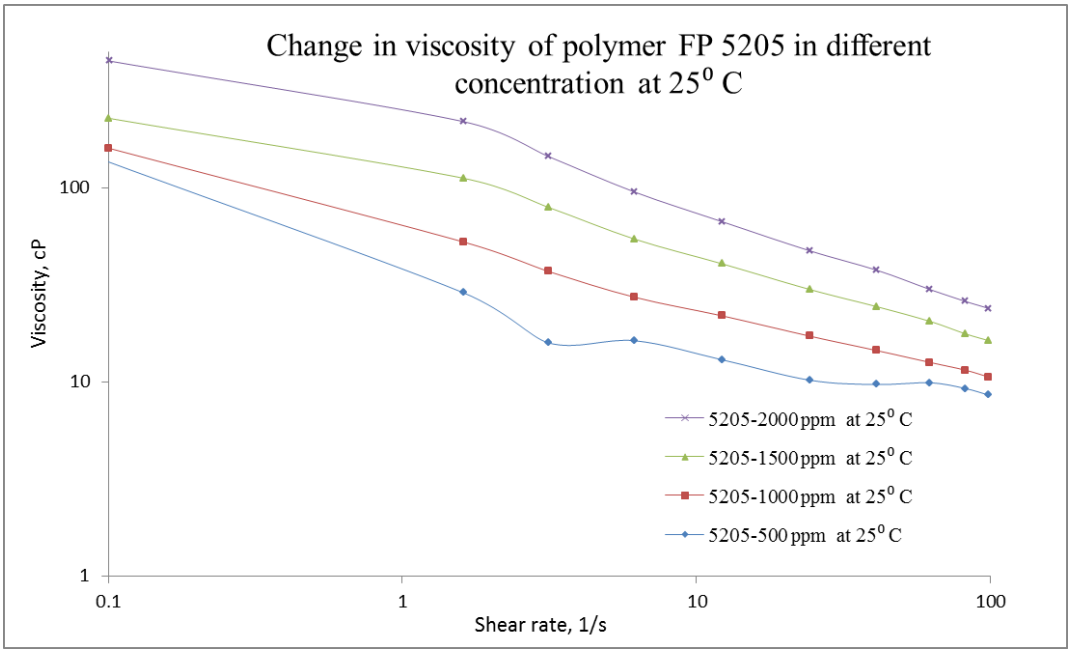

Figure 5.2 Rheological data of polymer FP5205 (log-log chart)

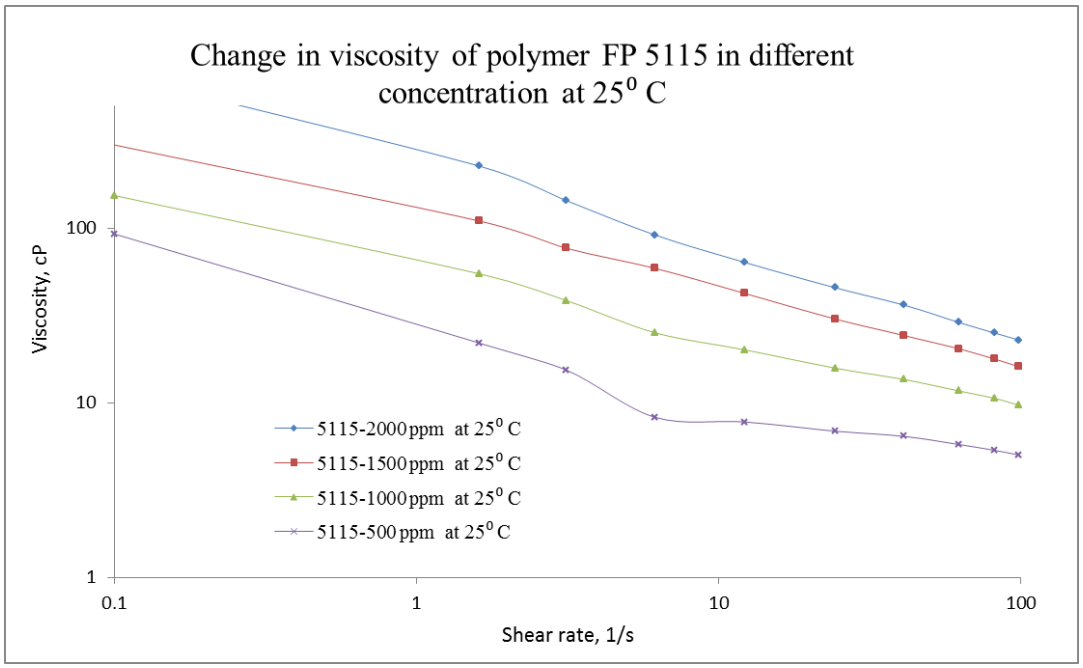

Figure 5.3 Rheological data of polymer FP5115 (log-log chart)

The polymer FP 5205 was chosen to conduct the main experiment as it has optimal properties: average molecular weight and average diameter of polymer's molecule. If the polymer FP 3630 would be chosen the adsorbtion and IPV value will be to high due to high molecular weight and as result large molecules, even if it has the highest hydrolysis degree. And if the polymer FP 5115 would be chosen there is a possibility that due to small molecules the IPV effect would not be measured.

From the rheology results it is noticed that for the lowest concentration – 500 ppm of all 3 polymer solutions, the curves are instable. This phenomena may be described by the idea that there can be some errors by measuring low viscosity solutions by rheometer Anton Paar MCR502.

5.2 Results of core analyses

Table 5.2 Results of standard analysis of core samples

No	Name of sample	Sampling depth, m	Dry weight of sample, g	Volume of plug, cm^3	Length of sample, cm	Diameter of sample, cm	Volume of sample grain, cm^3	Pore volume, cm^3	Porosity, %	Bulk density of rock, g/cm^3	Mineralogical density of rock, g/cm^3	Gas permeability, mD
1	Akkudyk 20	2253.24	41.65	21.51	3.18	2.93	15.80	5.71	26.6	1.94	2.64	687.6
2	Akkudyk 19	1920.34	41.28	21.30	3.19	2.92	15.67	5.64	26.5	1.94	2.63	552.4
3	Botakhan	1705.4	43.11	21.81	3.19	2.95	16.34	5.47	25.1	1.98	2.64	604
4	Akshabulak 45	1777.3	40.7	21.5	3.17	2.94	15.34	6.15	28.6	1.89	2.65	321.80
5	Akshabulak 206	1883.37	43.6	21.6	3.18	2.94	16.54	5.02	23.3	2.02	2.63	891.10
6	Akshabulak 501	1656.59	106.88	50.02	4.50	3.76	40.31	9.71	19.4	2.14	2.65	1210.00

After measuring the total porosity, permeability and pore size distribution, it was decided to use core plug #6. As it has the highest gas permeability -1210 mD, even the porosity is not highest, the pore size distribution, comparing to others is quite good, 62.3%of pores are belong to the pores from 1 to 50 μm. (Figure 5.1). Other core plugs' pore size distributions are presented in Appendix B.

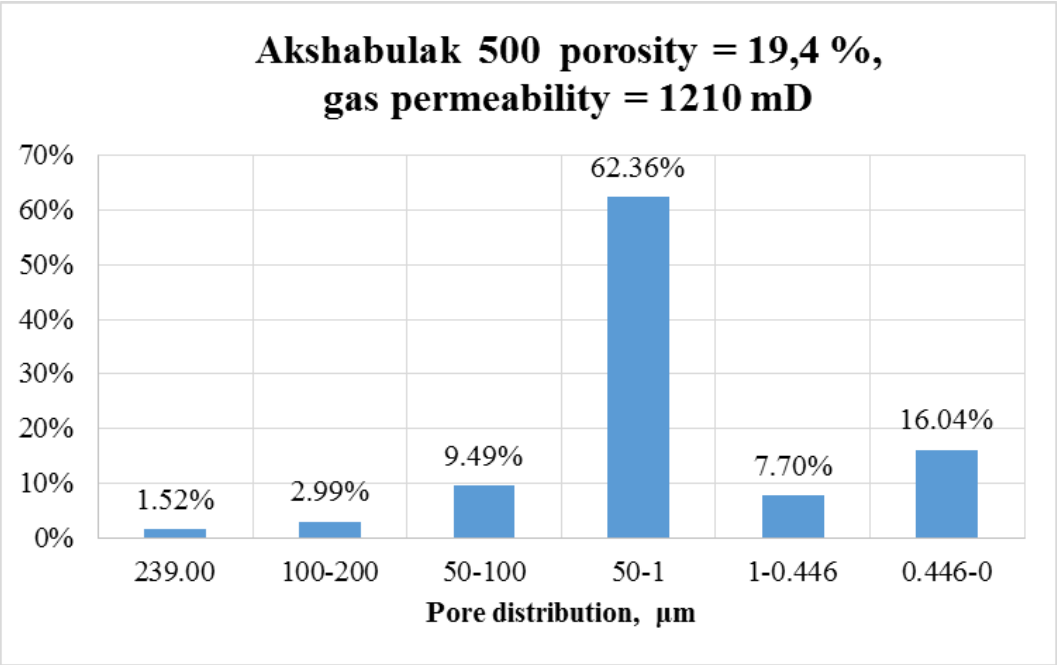

Figure 5.4 The pore size distribution of core plug Akshabulak 501

5.3 Results of main experiments

The plots of tracer and polymer curves are shown in figure 5.5 and 5.6 respectively. The pore volume at the x-axis is equal to the multiplication of flow rate to the total time and divided by pore volume of core plug, which is equal to the 9.71 cm^3 (Table 5.2).

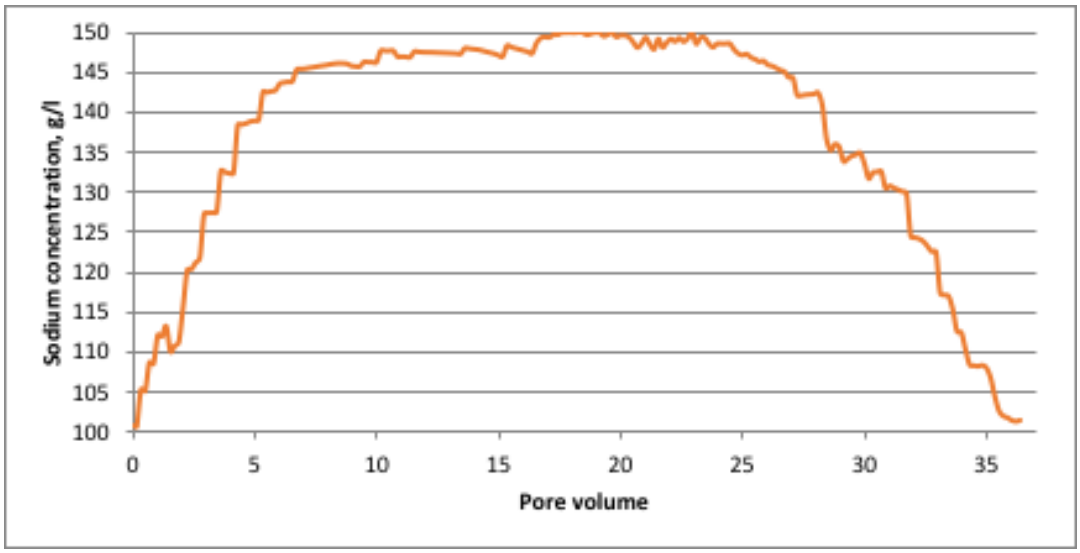

Figure 5.5 Tracer effluent curve

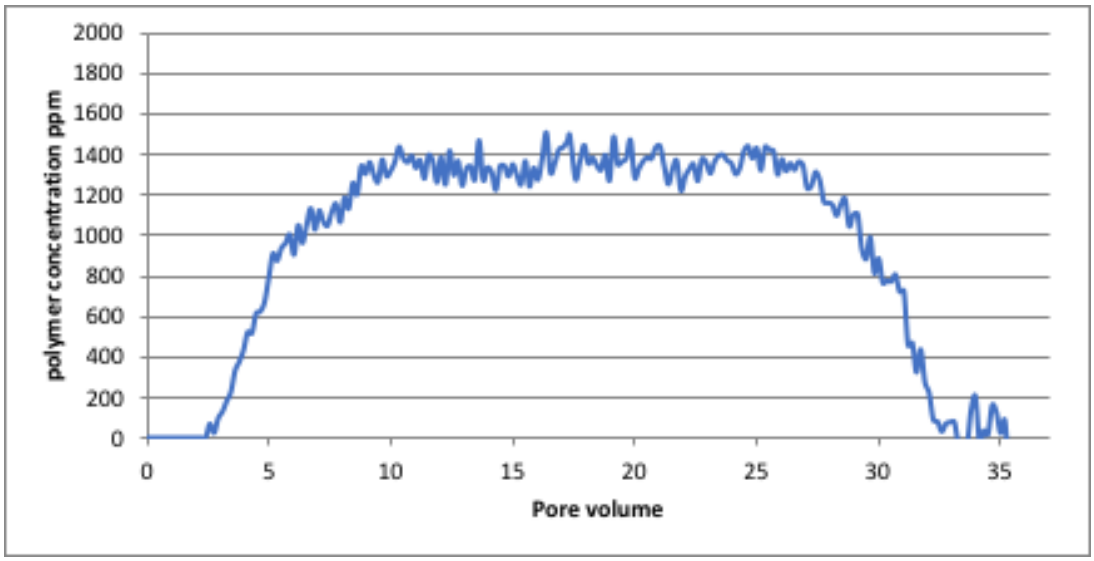

Figure 5.6 Polymer effluent curve

The normalized concentration of each curve is presented on figure 5.7. The normilized concentration was calculated according to equation 3.1.

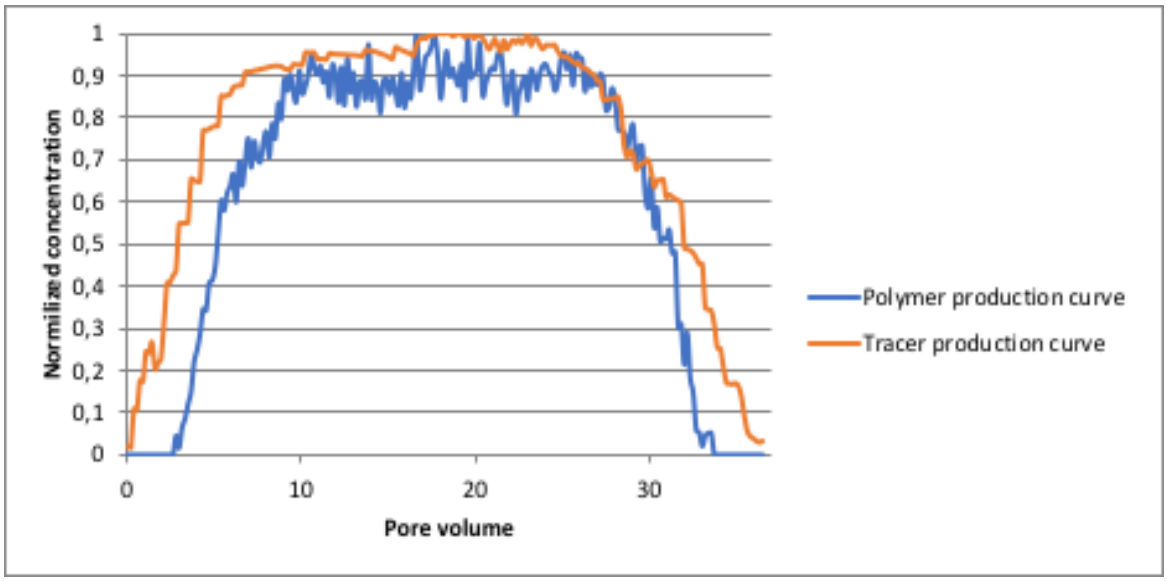

Figure 5.7 Effluent curves

The adsorption and IPV values were calculated according to equations 3.2 and 3.3. (Table 5.3) To determine the integral between the tracer and the polymer curve while the polymer injection and integral between the tracer and the polymer curve during the water injection after the polymer injection the MATLAB software was used. (Figure 5.8). The code is shown in Appendix D.

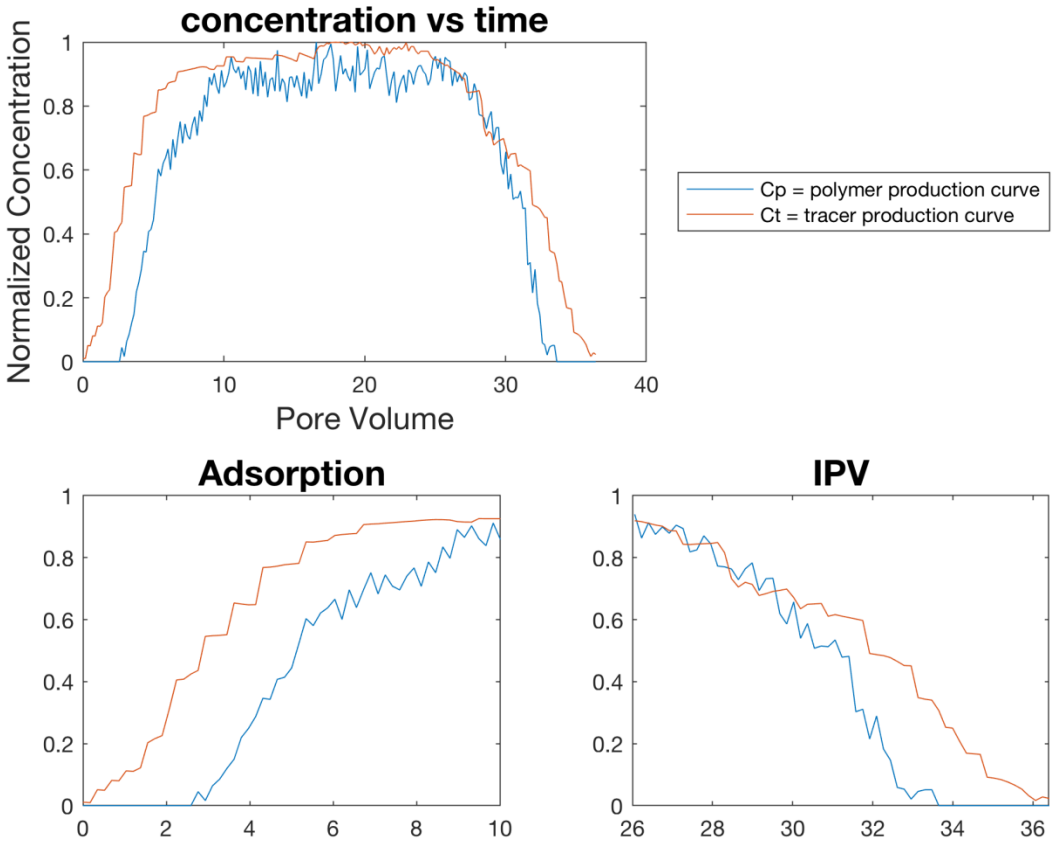

Figure 5.8 Calculation IPV and adsorption

Table 5.3 Calculated IPV and adsorption for core plug - Akshabulak 501

	Value
Weight of sample, g	106.88
Volume of sample, cc	50.02
Pore volume of sample, cc	9.71
Total porosity of sample, %	19.4
IPV	**14.8**
Adsorption, g/g	**0.0006**
Polymer adsorbed, g	**0.064**

According to the conducted research it should be mentioned that the concentration of effluent polymer is not equal to the concentration of injected polymer. If the concentration of injected polymer was 2000 ppm, the maximum

concentration of effluent was around 1500 ppm. This phenomenon may be explained by the fact of the mechanical destruction during polymer flow through porous media and permanent trapping of the larger molecules of polymer between the core's grains. Also, the concentration of polymer curve at the beginning and the end of the experiment reached values close to zero, but did not go down to zero. This fact can be most likely due to sensitivity of pressure transducers, as the tracer viscosity is very low it is very problematic to record pressure gradient inside the coil tube. The same behavior was noticed in tracer curve, which can be explained by the dissolving of salts from core's grains.

Another interesting conclusion is the fact that IPV is 14.8%, while according to the pore size distribution the percentage of pores that was smaller than the diameter of polymer is 16%. Even if these numbers are not equal they are pretty close and the difference can be attributed to the polydispersity of the actal polymer solution. Additionally, the difference between these two numbers may be due to a discrepancy between the measured pore size distribution and the pore size distribution in the actual core, as for the former measurement (mercury porosimetry) a small part of core was taken.

Chapter 6 – Comparison with numerical modelling

To help understand the phenomena happening during polymer solution flow through core sample, a multi-scale model was implemented in MATLAB. The code was written based on the scientific paper of Papathanasiou et al - "Dynamic Modeling of mass transfer phenomena with chemical reaction in immobilized-enzyme bioreactors" (Papathanasiou, 1988). Although the paper is for the fluid bed immobilized – enzyme bioreactors, it includes the important parameters to describe the behavior of polymer solution in porous media containing multi-scale porosity. These are mass transfer and diffusion characteristics, as well as a first-order intraparticle chemical reaction. The model considers the following factors:

- mass accumulation and consumption in intrapracticle space
- mass diffusion into the pore spaces
- Uniformity of species activity all over particles
- stationary particles

The model is used to take into account diffusion/reaction inside the small grains (or within the microscale porosity) that are described using ordinary equations which can be easily solved in MATLAB. The diffusion of a species within the grains (bead) is impacted by a combination of these factors, in dimensionless form, typical values are given in square brackets:

- D_R - dimensionless diffusivity, to describe how accessible the reactant is diffuse to the particles [10^{-4} to 50]
- β – Partition coefficient to describe the partitioning of a substance between the bulk and the intrapracticle space
- B_m -Biot number, describes how effectively the reactant travels from the solution to the particles [0.01 to 100]
- P_e - Peclet number, ratio of the superficial fluid velocity and the reactor length to the axial dispersion
- e- bed voidage, ratio of empty space to total volume of the column
- e_p – particle voidage, ratio of empty space to volume of the bead
- ϕ -Thiele Modulus, a measure of how fast the reaction occurs [0 to 10].

In accordance with dispersion model presented in the paper the mass balance in the bulk liquid (dimensionless) is:

$$\frac{\partial C_L}{\partial t_R} = \left(\frac{1}{P_e}\right)\left(\frac{\partial^2 C_L}{\partial x^2}\right) - \left(\frac{\partial C_L}{\partial x}\right) - Q^*, \qquad (6.1)$$

where

C_L- concentration in the bulk liquid

Q^* - fluid to particle mas flux, $Q^* = 3\,(1-\varepsilon)[\frac{D_{eff}}{R(\frac{F}{V_T})}]\,\left(\frac{\partial C_R}{\partial r}\right)_{r=R}$

t_R = dimensionless time, $\frac{t}{\varepsilon}\left(\frac{F}{V_T}\right)$

P_e = Peclet number, dimensionless, uL/D_L

x = dimensionless axial distance

The relation between the concentration at the particle surface (C_R) and the concentration in the bulk liquid (C_L) is determined by the method outlined in the publication. After discretization of Equation (6.1) into N nodes, the set of ODEs for node "i" are given by the following equations where n = 1, 2 … n0.

$$\frac{\partial C_i}{\partial t_R} = \left[\left(\frac{1}{P_e \delta x^2} + \frac{1}{2\delta x}\right) C_{j-1} - \left(\frac{2}{P_e \delta x^2} + 3(1-\varepsilon) B_m D_R\right) C_i + \left((3(1-\varepsilon) B_m D_R)\right) \beta C_{Ri} + \frac{\varepsilon D_R}{S_i}\, C_{j+1}\right], \quad (6.2)$$

$$\frac{dC_{Ri}}{dt_R} = \frac{B_m}{2\varepsilon_p}\frac{\varepsilon D_R}{S_i} C_i - \frac{\varepsilon D_R \beta}{S_i}\left(\frac{9\phi^2 S_i}{\beta} + \frac{B_m}{2\varepsilon_p}\right) C_{Ri} - \frac{\varepsilon D_R}{S_i} \sum_{1}^{n_o} \Psi_i^n, \quad (6.3)$$

$$\frac{d\Psi_i^n}{dt_R} = \left[\frac{B_m}{2\varepsilon_p}\frac{\varepsilon D_R}{S_i} C_i - \frac{\varepsilon D_R \beta}{S_i}\left(\frac{9\phi^2 S_i}{\beta} + \frac{B_m}{2\varepsilon_p}\right) C_{Ri} - \frac{\varepsilon D_R}{S_i} \sum_{1}^{n_o} \Psi_i^n + 9\varepsilon D_R \phi^2 C_{Ri} - (9\varepsilon D_R \phi^2 + \varepsilon D_R \pi^2 n^2) \Psi_i^n\right], \quad (6.4)$$

The resulting system of N(2+n0) ODEs can be solved using standard ODE solvers in MATLAB.

Based on the dynamic model, figure 6. 1 shows how varying the diffusivity

values affect to the concentration profile of the effluent. Case 1 has a D_r=0.0001 – low enough that the species does not diffuse within the particles of the immobilized bed. The rapid increase in concentration is explained by the fact that molecules hop between small spaces between particles since, due to its larger molecule size it cannot diffuse into the micro-porous space, and therefore spreading takes short time. Case 2 (D_r=50), on other hand, corresponds to molecules which easilty diffuse into the micro-porous space (in our case, smaller molecules) , and as a result we observea slower increase in effluenet concentration. In this case, polymer molecules have to travel through the entire, micro- and macro-porous space before exiting the sample.

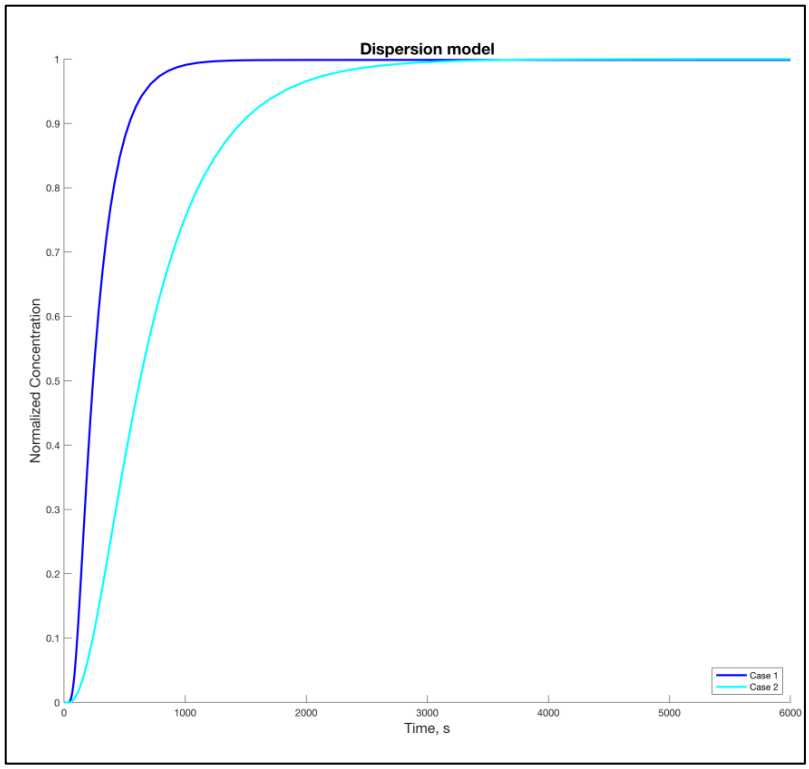

Figure 6.1 Comparing low Dr (pure dispersion case) and high Dr (diffusion in particles impacts the response) cases

Case	n	N	D_r	B_m	β	ϕ	P_e	e	e_p	delay
1	25	100	0.001	1	1	0	3	0.3	0.7	0
2	25	100	10	1	1	0	3	0.3	0.7	0

To compare the predicted response to the experimental data, two 2 different regimes were studied: the rise (polymer injection) and fall (brine injection). Thus we can use modelling to helping explain what is happening during the core experiments: polymer and brine injection.

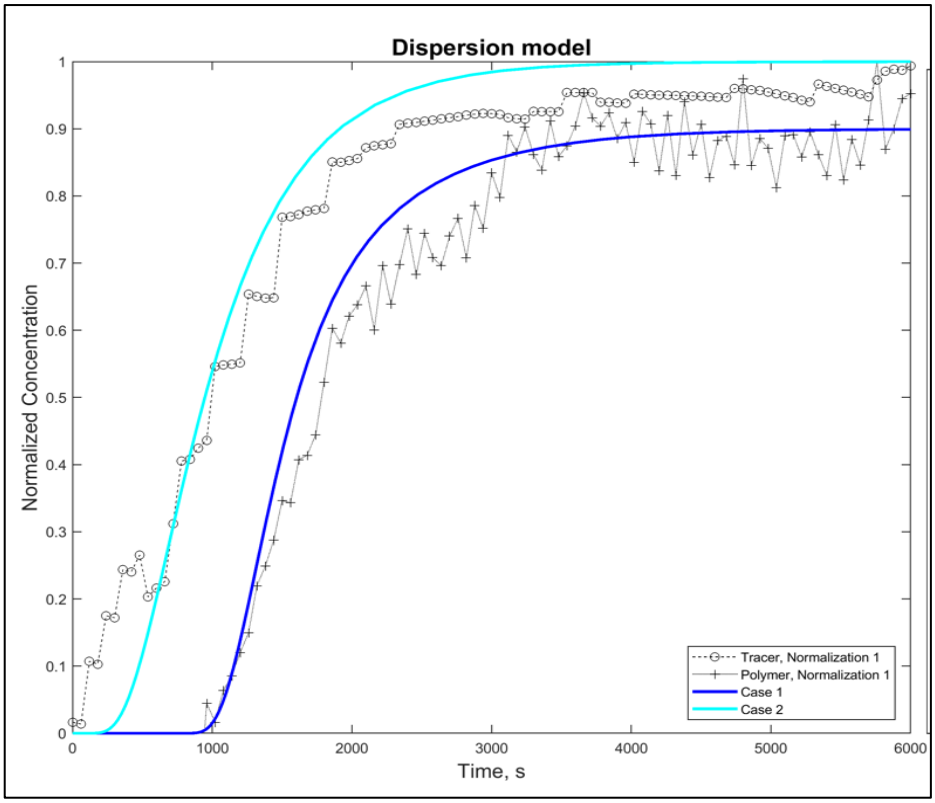

Figure 6.2 Modelling of tracer and polymer curve rise with delay

Case	n	N	D_r	B_m	β	ϕ	P_e	e	e_p	delay
1	25	100	0.7	1	1	0.3	10	0.7	0.9	650
2	25	100	100	1	1	0	5	0.7	0.9	0

The parameters for tracer and polymer rising curve are compared in figure 6.2. The delay of polymer curve takes place due adsorption to the grain. The

adsorption of the polymer solution is characterized by the capture of the polymer by small pores (dynamic adsorption) and the deposition of the polymer on a solid pore surfaces (static adsorption). We can assume that these phenomena can be approximated by a first order reaction between polymer solution and particles and take $\varphi = 0.3$ (a good fit with experimental data was obtained using this value). As it is noticed from figure 6.2 polymer species corresponds to the lower diffusion (fit with low D_r and high P_e values), whereas the tracer to a higher amount of diffusion (fit with high D_r and low P_e values). The diffusion of polymer in porous media is governed by the heterogeneity of the core sample, especially by multi-scale porosity. The diffusion for polymer species is associated with inaccessible pore volume effects that accelerate the polymer solution through a permeable medium. The relation between Peclet number and diffusion is indicated by the fact that low Peclet number corresponds to large values of diffusivity whereas high Peclet number – smaller values of diffusivity (Kirby, 2010).

In our case, the fast molecular diffusion of the tracer can be explained by the fact that tracer accessibly flows through core plugs due to its small molecule size. Polymer agent, in other hand, is not accessible to the particles due to the IPV effect, and therefore the diffusivity is low.

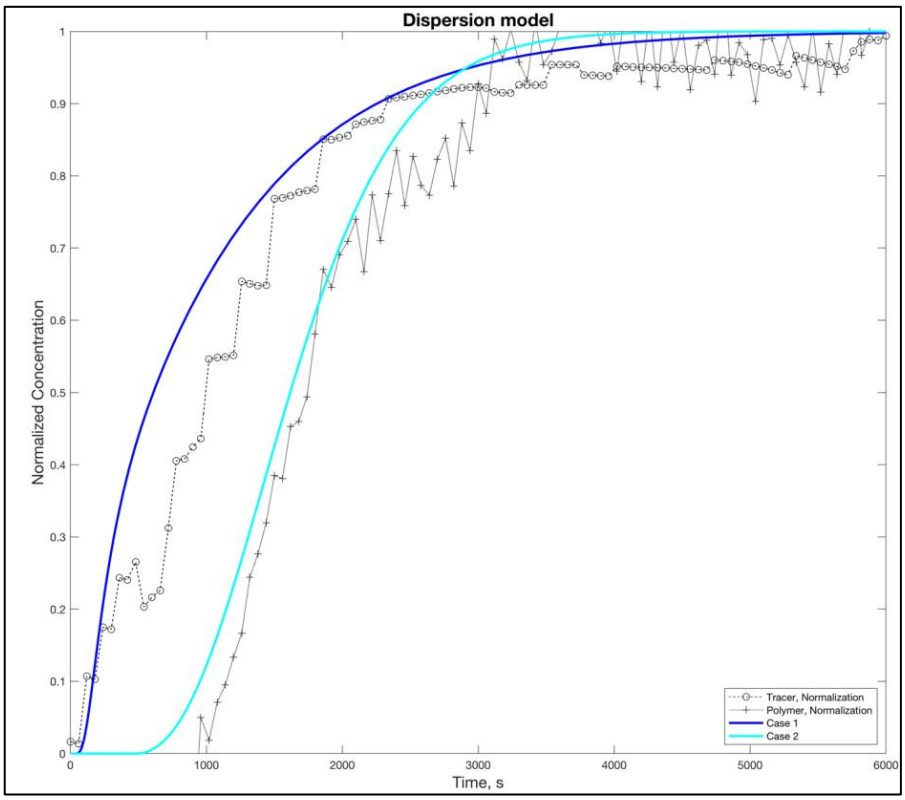

Figure 6.3 Modelling of tracer and polymer curve rise without delay

Case	**n**	**N**	**D_r**	**B_m**	**β**	**ϕ**	**P_e**	**e**	**e_p**	**delay**
1	25	100	10	0.1	0.2	0	3	0.4	0.2	0
2	25	100	4	1	0.15	0	500	0.4	0.2	0

Figure 6.3 represents the same experimental data of polymer and tracer rise but with another set of parameters. As it seen from the figures (6.2 and 6.3) the main concept related to the diffusion is remain the same: polymer species corresponds to the low diffysivity and high Peclet namber, while the tracer curve is opposite. However the varied coefficient here are β (partition coefficient) and delay. For figure 6.2 the delay parameter should be increased to 650 s for polymer solution, to shift it a bit to the right, show delay and fit experimental data. Even if considering that before take the measurement the species need to flow through the long coil the delay should be only 80 seconds. Also according to the scheme

(figure 4.4) both polymer and tracer have to flow through the coil together, before recording the values. Therefore, implementing the delay here is not reasonable.

Moving to the figure 6.3 it is seen that delay for both cases are the same, however β is less than 1, and different for both cases. These discrepancies can arise due to the fact that the porous core sample is not exactly the same as a fixed-bed reactor or an assembly of porous spheres. But still the main concept of diffusion/reaction inside small grains taking into account micro scale porosity is confirmed and explained.

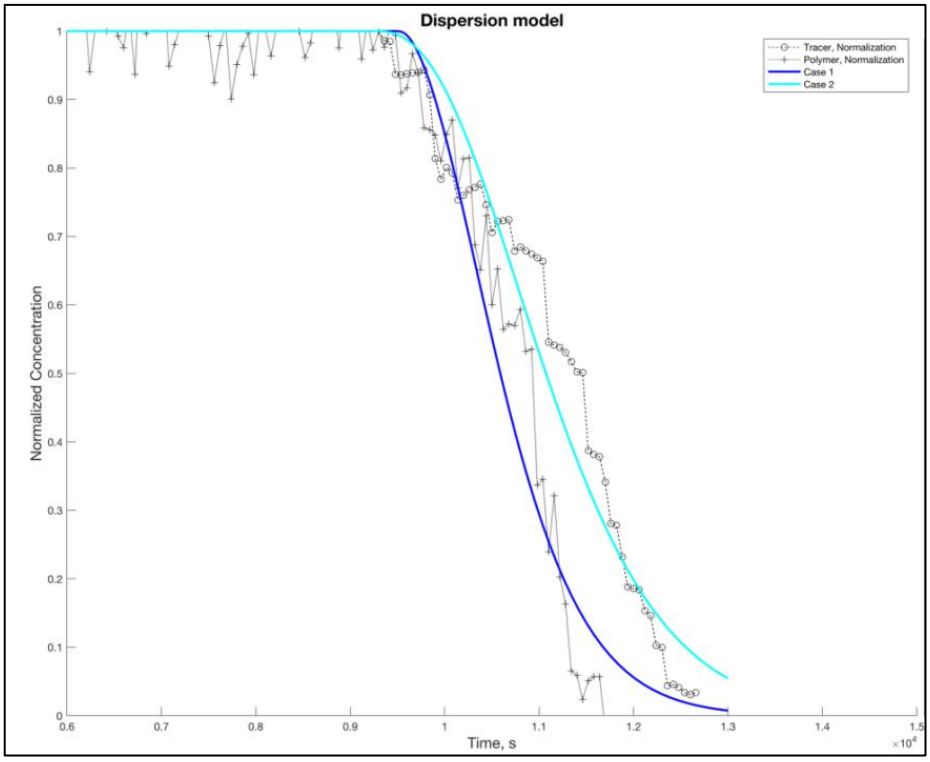

Figure 6.4 Modeling the polymer and tracer fall curve

Case	**n**	**N**	**D_r**	**B_m**	**β**	**ϕ**	**P_e**	**e**	**e_p**	**delay**
1	25	100	10	0.1	0.2	0	3	0.4	0.2	0
2	25	100	4	1	0.15	0	500	0.4	0.2	0

Although, for the falling curves (figure 6.4), a set of parameters that will fit the experimental data with β=1 was not found, the main concept is still the

same. As in rise curves, here the tracer species have the higher molecular diffusion than polymer, which is confirmed with high D_r value and low Peclet number for tracer curve. The reason why polymer comes out faster than the tracer is the IPV. The inaccessible pore volume depends on the molecular weight of the polymer, the permeability, the porosity and the pore size distribution of core plug sample. Considering the fact that polymer molecules' diameter much bigger than tracer's and core plug is characterized by a multi – scale porosity, the polymer molecules are incapable to flow through whole pore volume of the core plug and consequently skip some of the pore volume which leads to a faster exit.

Summarizing this chapter, a dynamic model to describe the transport of polymer through a multi – scale porous media from the literature was compared to the experimental curves obtained from a core sample. Even though it is difficult to assign physical values to all model parameters, the idea of diffusion in multi scale porosity medium, which is central to the model, seems to explain the difference between polymer and tracer effluent curves. Two key parameters to reproduce the shape of the experimental curves, the Peclet number and dimensionless diffusivity, were identified. At low values of diffusivity, as is the case for the polymer molecules, part of the core sample is rendered inaccecible to the polymer, thus reproducing the IPV effect.

Chapter 7 - Conclusion

Based on the results of this master thesis including all experimental and numerical work the following conclusions can be drawn:

- Polymer flooding has a future in Kazakhstan's oil fields as the 62.7 % of them are on the last stage of the production, and according to the world experience it has a wide range of criteria to apply.
- To successful injection of polymer solution in reservoirs its transport behavior in porous media need to be studied properly. Two main factors that have a great impact on that is inaccessible pore volume (IPV) and polymer retention that includes adsorption on the grain surface.
- Tracer, as sodium chloride, was used to contrast the polymer flow. And the IPV and adsorption was measured during core flood experiments and found by effluent concentration of polymer and tracer. The results show that adsorption is 0.0006 g\g, polymer adsorbed is 0.064 g, the core sample's inaccessible pore volume for polymer solution is 14.8 % while the pore diameter less than polymer molecule is 16%. Even these number are not the same, they are pretty close, what confirm the theory that IPV effect takes place due to skipping the polymer molecules small pore sizes.
- A dynamic model to describe the transport of polymer through porous media was presented. According to the model, it is highlighted that there is

now ideal case that would fit and explain totally the experemetal data. This can happen due to the fact that porous media of core sample is not a fixed bed – reactor. It was confirmed that polymer molecules have lower diffusivity than tracer molecules. The most important parameters are found to be the Peclet number and the dimensionless diffusivity. This phenomena may be explained by the fact that polymer‘s molecules hop between grains due to their large size (thus avoiding the IPV), while tracer molecules, beign smaller, can travel through the entire micro- and macro-scale pore space.

References

1 A. Stavland, H. J., 2010. Polymer Flooding – Flow Properties in Porous Media Versus Rheological Parameters. Barcelona, Spain, Society of Petroleum Engineers.

2 Abou-Kassem, J. H., 1999. Screening of Oil Reservoirs for Selecting Candidates of Polymer Injection. 21:5(16).

3 Aluhwal, H., Omar, K., 2008. Simulation Study of Improving Oil Recovery by. polymer flooding in Malaysian reaservoir. Faculty of Chemical and Natural Resources Engineering, Universiti Teknologi.

4 Anon., 2012. Applicability of selected EOR techniques. Shell's EOR brochure, p. 8.

5 Available at: https://kapital.kz/econom ic/40889/nefti-stanet-bolshe.htm l

6 Berkowitz, B. & Scher, H., 2000. Anomalous transport in laboratory-scale, heterogeneous. WATER RESOURCES RESEARCH, VOL. 36, pp. 149-158.

7 Bijeljic, B. & Blunt, M. J., 2006. SPE Annual Technical Conference and Exhibition. San Antonio, Texas, USA, Society of Petroleum Engineers, pp. 24-27.

8 Brigham, W., 1974. Mixing Equations in Short Laboratory Cores. Society of Petroleum Engineers Journal, Issue 14.

9 Bulekbai, A., 2013. Problems of mature reservoirs in Republic of Kazakhstan or the second life opportunity. Kazenergy, p. 57.

10 Chang, H. Z., 2006. Advances in polymer flooding and alkaline/surfactant/polymer processes as developed and applied in the People's Republic of China. 58(2).

11 Chauveteau, G., 1982. Rodlike Polymer Solutions Flow Through Fine Pores: Influence of Pore Size on Rheological Behavior. Journal of Rheology, 26(2), pp. 111- 142.

12 Chauveteau, G., Denys, K. & Zaitoun, A., 2002. New Insight on Polymer Adsorption Under High Flow Rates. Tulsa, Oklahoma, SPE/DOE Improved Oil Recovery Symposium.

13 Coats, K. H. & Smith, B. D., 1964. Dead end pore volume and dispersion in porous media. Society of Petroleum Engineer Journal, pp. 73-84.

14 Daniel Broseta, 1995. Polymer Adsorption/Retention in Porous Media: Effects of Core Wettability and Residual. SPE Advanced Technology Series, 3(1), pp. 103-107.

15 Dawson, R. & Lantz, R. B., 1972. Inaccessible Pore Volume in Polymer Flooding. Society of Petroleum Engineers Journa, Issue 12, pp. 448-452.

16 Dawson, R. & Lantz, R., 1972. Inaccessible Pore Volume in Polymer Flooding. SPE Journal, 12(5), p. 448–452.

17 Delamaide, E. B., 31 March-2 April 2014. Chemical EOR for Heavy Oil:the Canadian Experience. Muscat, Oman, SPE 169715 presented at the SPE EOR Conference at Oil and Gas West Asia.
18 Diaz-Viera, M., Lopez-Falcon, D., Moctezuma-Berthier, A. & Ortiz-Tapia, A., 2008. COMSOL Implementation of a Multiphase Fluid Flow Model in Porous Media. Boston, U.S.A, б.н.
19 Don W. Green, G. P. W., 1998. Enhanced Oil Recovery. Richardson, Texas: Society of Petroleum Engineers.
20 Ferreira, V. H. S., Moreno R. B. Z. L., 2016. Modeling and Simulation of Laboratory-Scale. Modeling and Simulation of Laboratory-Scale, Issue 16, pp. 24-33.
21 Flory, P. J., 1953. Principles of Polymer Chemistry. б.м.:Cornell University Press
22 Genuchten, M. V. & Wierenga, P., 1976. Mass transfer studies in sorbing porous media I. Analytical solutions, Soil Science Society of America Journal, pp. 473-480.
23 Gupta, S., 1978. Micellar Flooding The Propagation of the Polymer Mobility Buffer Bank. Society of Petroleum Engineers Journal, Issue 18, pp. 5-13.
24 Hatzignatiou, D. G., Norris, U. L. & Stavland, A., 2013. Core-scale simulation of polymer flow through porous media. Journal of Petroleum Science and Engineering, 108, pp. 137-150.
25 Hatzignatiou, D., Moradi, H. & Stavland, A., 2013. Experimental Investigation of Polymer Flow through Water- and Oil-Wet Berea Sandstone Core Samples. London, United Kingdom, Society of Petroleum Engineers.
26 Hatzignatiou, D., Norris, U. L. & Stavland, A., 2013. Core-scale simulation of polymer flow through porous media. Journal of Petroleum Science and Engineering, 108, pp. 137-150.
27 Huh, C. , 1990. Polymer Retention in Porous Media. Tulsa, Oklahoma, U.S.A., Society of Petroleum Engineers, pp. 567-586.
28 Huysmans, M. & Dassargues, A., 2005. Review of the use of Peclet numbers to determine the relative importance of advection and diffusion in low permeability environments. Hydrogeology Journal, Vol. 13, pp. 895-904.
29 Idahosa, P. e. a., 2016. Rate-dependent polymer adsorption in porous media. Journal of Petroleum Science and Engineering, pp. 65-71.
30 Joseph C. Trantham, P. D. M., 1982. North Burbank Unit 1,440-Acre Polymer Flood Project Design. Tulsa, Oklahoma, SPE Enhanced Oil Recovery Symposium.
31 Juri, J. E., Ruiz, A. M., Hernandez, M. I. & S. Kaminszczik, 2015. Estimation of Polymer Retention from Extended Injectivity Test. Kuala Lumpur, Malaysia, Society of Petroleum Engineers.

32 K. Kamalyar et al, 2014. Numerical Aspects of the Convection-Dispersion Equation. Petroleum Science and Technology, 32, p. 1729-1762.
33 Kiinov, L. K., 1994. Features of the development of paraffin and viscous oil fields in Western Kazakhstan in the context of the implementation of energy-saving technologies, Moscow, Russia,VNIIneft.
34 Kirby, B., 2010. Micro-and NanoscaleFluidMechanics. б.м.:Cambridge University Press.
35 Kolodziej, E. J., 1988. Transport mechanisms ofxanthan biopolymer solutions in porous media. Houston, Texas, Proceedings of the 63rd Annual Fall Conference ofSPE.
36 Koval, E. J., 1963. A method for predicting the performance of unstable miscible displacements. Society of Petroleum Engineers Journal, pp. 145 - 154.
37 Lake, L., 2010. Enhanced oil recovery. Texas, USA: The Society of Petroleum Engineers.
38 Lötsch, T. M, Muller T & Pusch G, 1985, The Effect of Inaccessible Pore Volume on Polymer Coreflood Experiments. Phoenix, Arizona, Society of Petroleum Engineers.
39 Martin, F.D., 1975, The effect of hydrolysis of polyacrylamide on solution viscosity, polymer retention and flow resistance properties, Society of Petroleum Engineering.
40 Moe, E. S., 2015. An Experimental and Numerical Study of Polymer Injection in Layered Synthetic Porous Media, Trondheim, Norway: Norwegian University of Science and Technology.
41 Moffitt, D. Z., 1993. Application of Freshwater and Brine Polymer Flooding in the North Burbank Unit, Osage County, Oklahoma. 8(02).
42 Moore, W. J., 1963. Physical chemistry. 4th edition ред. London: Longman. Norris, U. L., 2011. Core-Scale Simulation of Polymer Flow through Porous Media. Stavanger: University of Stavanger.
43 Nadirov, N. K., 1982. New oils of Kazakhstan and their use. Enhanced oil recovery technology, Almaty, Kazakhstan, "Наука" Journal.
44 Osterloh, W. T. & Law, E. J., 1988. Polymer Transport and Theological Properties for Polymer Flooding in the North Sea Captain Field. Tulsa, Oklahoma, U.S.A, Society of Petroleum Engineers,.
45 Pancharoen, M., Thiele, M. R. & Kovscek, A. R., 2010. Inaccessible Pore Volume of Associative Polymer Floods. Tulsa, Oklahoma, USA, SPE Improved Oil Recovery Symposium.
46 Papathanasiou, T.D., Kalogerakis, N. & Behie, L.A., 1988. Dynamic Modelling of Mass Transfer Phenomena with Chemical Reaction in Immobilized-Enzyme Bioreactors. Chemical Engineering Science, 43(7), pp. 1489-1498.

47 Perkins, T. & Johnston, O., 1963. A Review of Diffusion and Dispersion in Porous Media. Society of Petroleum Engineers Journal, Issue 3, pp. 70-84.
48 R.N. Manichand, N. a. R. S., 2014. Field vs Laboratory Polymer Retention Values for a Polymer Flood in the Tambaredjo Field. Tulsa, Oklahoma,, Society of Petroleum Engineers, p. U.S.A. T.
49 Seright, R. S., Fan, T., Wavrik, K. E. & Balaban, R. D. C., 2010. New Insights into Polymer Rheology in Porous Media. Tulsa, Oklahoma, USA, SPE Improved Oil Recovery Symposium.
50 Shah, B. D., 2012, Improved Oil Recovery by Surfactant and Polymer Flooding. Kansas City: Elsevier Inc., pp. 511-554.
51 Sorbie, K. & Phill, D., 1991. Polymer - Improved Oil Recovery. New York: Springer Science+Business Media, LLC.
52 Sorbie, K., Parker, A. & Cfifforrf, P., 1987. Experimental and Theoretical Study. SPE Reservoir Engineering.
53 Statistics, C. o., 2014. GDP, s.l.: Ministry of National Economy of the Republic of Kazakhstan Committee on Statistics.
54 Taber, J.J., Martin, F. D., Seright, R. S., 1997. EOR Screening Criteria Revisited—Part 2: Applications and Impact of Oil Prices, SPE Reservoir Engineering journal, 12(03).
55 Taber, J.J., Martin, F. D., Seright, R. S., August 1997. EOR Screening Criteria Revisited- Part 1: Introduction to Screening Criteria and Enhanced Recovery Field Projects, SPE Reservoir Engineering journal, 12(03).
56 Tumasheva, E., 2015. kapital.kz. [Online]
57 Wan, H. & Seright, R. S., 2016. Is Polymer Retention Different Under Anaerobic vs. Aerobic Conditions?. Tulsa, Oklahoma, U.S.A., Society of Petroleum Engineers.
58 Wang, D. H. P. S. Z. W. H. S. R., 2008. Sweep improvement options for the Daqing oil field. 11(01).
59 Wang, D., Seright, R. S., Shao, Z. & Wang, J., 2008. Key Aspects of Project Design for Polymer Flooding at the Daqing Oilfield. SPE Reservoir Evaluation & Engineering, Issue 11, pp. 1117-1120.
60 Willhite, G. P. , Dominguez, J. G., 1977, Mechanisms of polymer retention in porous media, Improved Oil Recovery by Surfactant and Polymer Flooding, pp 511-554.
61 Womersley, J., 1955. Method for the calculation of velocity, rate of flow and viscous drag in arteries when the pressure gradient is known. The journal of Physiology, 127(3), pp. 553-563.
62 Zhang, G. & Seright, R., 2015. Hydrodynamic Retention and Rheology of EOR Polymers in Porous Media. Texas, USA, SPE International Symposium on Oilfield Chemistry.

Appendices

Appendix A

Appendix A presents worldwide experience of polymer flooding and effect of this.

Figure A. 1 World experience of polymer flooding

Field, country	Operating company, year	Depth, m	Thickness, m	Area, ga	Temperature, ^{0}C	Porosity, %	Lithology	Oil viscosity,cP	Permeability, mD	Salinity of injected water, %	Polymer and it concentration, %	Effect
1	2	3	4	5	6	7	8	9	10	11	12	13
Niagara fiels, Kentuki, USA	Dou Chemical, 1959	-	-	-	-	-	sandstone	16	20		вязкость раствора 1,35 мПа*с	Oil production increase
North Hosvill, Texas	Hant oil chemical ,1963	-	-	2800	105	-	Limestone	0,07-0,09	50	-	Pusher, 0,025-0,05	+3.3% increase in oil production
Vernon, Cansas	1963	-	-	6	24	-	-	75	30	-	Pusher, 0,045	+8.6% increase in oil production
Nightingto beach, California	Стандарт Оил К, 1964	-	-	3600	52	-	-	37-76	2300	-	Pusher, 0,05-0,035	4.1% increase in oil production
Brea Olinda, California	1967	-	-	9,6	57	-	-	25-100	750		Pusher, 0,08	Increase in oil production
Tiber Saut	Ashland Pan. Can. Pet., 1967	990	22	364	35	26,3 26.6	Sandstone	58	2100	Mixture of fresh water and brine	Pusher-500 и Pusher-700, 0,036 or 0,023	-
Scal-Krick	1967	-	-	222	51	-	-	3,2	70	-	Pusher -500, 0,024	+8.2% increase in oil production
Orlyanskoe, south part, Russia	Cuibyshev neft (1968 - 1976)	960 - 1050	6,0	-	24	19 - 25	Sandstone-limestone	9-14	400-1300	1-2 g/l	PAA, 0,01 - 0,015	1832 t of addition oil production to 1t on the injected agent
Orlyanskoe, north part, Russia	Cuibyshev neft (1973 - 1976)			282								1106 t of addition oil production to 1t on the injected agent
Brelam, 1969	Duved, Texcaco Inc.	595	3	107	44	29,3	sandstone	9,8	400	Mixture of fresh water and brine	Pusher-723, (0,0389-0,0075)	+8.6% increase in oil production
Wilmington, California	Mobil oil corparation, 1969	-	-	152	57	-	-	30,8	Very high	-	Pusher -700, 0,021	Not successful concentration of polymer and injection volume was low

1	2	3	4	5	6	7	8	9	10	11	12	13
North barbenk, Phillips	1970	914	11-15	64-65	47	11-32	sandstone ник	3,0	1000-2000	0,12	Pusher -1000, (0,025-0,0025)	+1.6% increase in oil production
Taber Manville, Alberta, canada Chevron	1971	960	9-10	208-210	33	23,2	Sandstone	120	1920	Fresh water	Pusher -700, 0,025	Noticed increase in oil production
Nof Alma	1971	-	-	52	52	-	-	29,5	110	-	Kelzan, 0,05	Decrease in watercut
Pembina, Alberta Canada, Mobil	1971	1524	4-5	128-130	52	7-13	Conglomerate, sandstone	1,1	450	0,025-0,03	Pusher -700, (0,1-0,01)	Not successful experiment due to small concentration of polymer and injected volume of agent.
West Semlek, Kruk, Waioming Terra Resources Inc.	1973	2205	8	139,2	62-63	20	sandstone	12,3	650	0,775	Betz (0,02)	+4.4 % increase in oil production
Ovasco unit, Kimbell, Nebrasca Chain Oil Inc.	1975	1845	-	207	77	17	sandstone	3,27	193	-	Calgon 454 (0,05-0,025)	
North Stanly osagz, Oklakhoma	1976	884	15,5	624 (404)	41	18	sandstone	2,2	300	Fresh water	Pusher -700, (0,0285)	48.4 t of addition oil production to 1t on the injected agent
North Stanly osagz, Oklakhoma	1977	600	4-6	44	-	30	sandstone	40	1000	0,05 g/l	PAA	Decrease in watercut
Kalamkas, kazakhstan	1981 - 1986	-	-	-	-		sandstone	20 - 25	Up to 5000	93 g/l		190t of addition oil production to 1t on the injected agent
Daging, Chine	PetroChina 1994	-	6-22	-	113	-	Sandstone-condlomerate	9	160-860	Low salinity	-	+4.420% increase in oil production

Appendix B

Appendix B presents the results of mercury porosimeter and pore size distribution.

The pore size distribution was calculated as the ration of delta volume of mercury of each step to the total intruded volume

Table B. 1Results of Mercury porosimeter of sample Akkudyk 20

Pressure [PSI]	Pore Diameter [nm]	Pore Diameter [µm]	Volume Intruded [cc/g]	Delta Volume [cc/g]	Volume Intruded %	Dv(d) [cc/(nm-g)]	dV/d(log [cc/g]	Pore size Distribution, %
1	2	3	4	5	6	7	8	9
0.815	261754	261.754	0	0	0	2.63E-08	1.65E-02	0
1.16	183896.6	183.8966	0.0021	0.0021	1.74	2.44E-08	1.03E-02	1.75
1.522	140139.5	140.1395	0.0032	0.0012	2.7	2.63E-08	8.53E-03	1.00
1.812	117752.7	117.7527	0.004	0.0007	3.33	3.51E-08	9.66E-03	0.58
2.352	90683.53	90.68353	0.0052	0.0012	4.35	8.00E-08	1.70E-02	1.00
2.785	76595.69	76.59569	0.0064	0.0012	5.35	6.94E-08	1.23E-02	1.00
3.795	56214.94	56.21494	0.0082	0.0018	6.87	1.90E-07	2.51E-02	1.50
4.415	48312.79	48.31279	0.0107	0.0025	8.93	4.55E-07	5.18E-02	2.09
5.246	40664.48	40.66448	0.0163	0.0056	13.59	1.17E-06	1.11E-01	4.67
6.241	34178.92	34.17892	0.0275	0.0112	22.92	2.01E-06	1.59E-01	9.35
7.208	29593.48	29.59348	0.037	0.0095	30.84	1.98E-06	1.35E-01	7.93
8.189	26050.71	26.05071	0.0446	0.0076	37.19	2.22E-06	1.33E-01	6.34
9.385	22730.78	22.73078	0.0506	0.006	42.19	1.56E-06	8.13E-02	5.01
10.406	20499.15	20.49915	0.0537	0.0032	44.82	1.36E-06	6.45E-02	2.67
11.806	18068.77	18.06877	0.057	0.0033	47.54	1.30E-06	5.39E-02	2.75
13.112	16269.08	16.26908	0.0592	0.0022	49.36	1.09E-06	4.09E-02	1.84
14.736	14475.79	14.47579	0.061	0.0019	50.93	1.14E-06	3.82E-02	1.59
16.419	12992.61	12.99261	0.0629	0.0018	52.44	1.33E-06	3.99E-02	1.50
17.966	11873.43	11.87343	0.0643	0.0014	53.64	1.21E-06	3.33E-02	1.17
19.561	10905.49	10.90549	0.0656	0.0013	54.7	1.39E-06	3.50E-02	1.09
21.325	10003.54	10.00354	0.0668	0.0012	55.69	1.25E-06	2.88E-02	1.00
23.155	9212.69	9.21269	0.0678	0.0011	56.57	1.48E-06	3.16E-02	0.92
25.069	8509.48	8.50948	0.0688	0.001	57.44	1.19E-06	2.31E-02	0.83
26.965	7911.04	7.91104	0.0694	0.0006	57.93	1.25E-06	2.28E-02	0.50
28.665	7441.78	7.44178	0.0702	0.0008	58.56	1.55E-06	2.66E-02	0.67
30.656	6958.66	6.95866	0.0709	0.0007	59.13	1.39E-06	2.24E-02	0.58
32.6	6543.65	6.54365	0.0713	0.0005	59.52	1.33E-06	2.02E-02	0.42
34.976	6099.05	6.09905	0.0723	0.0009	60.3	2.12E-06	2.99E-02	0.75
37.853	5635.54	5.63554	0.0731	0.0009	61.02	1.83E-06	2.38E-02	0.75
40.722	5238.5	5.2385	0.0739	0.0008	61.7	2.06E-06	2.48E-02	0.67
43.305	4926.05	4.92605	0.0745	0.0005	62.15	2.00E-06	2.29E-02	0.42
46.075	4629.9	4.6299	0.0752	0.0007	62.73	2.25E-06	2.41E-02	0.58
51.675	4128.16	4.12816	0.0771	0.0019	64.3	4.87E-06	4.72E-02	1.59
61.826	3450.38	3.45038	0.0812	0.0042	67.77	6.26E-06	4.96E-02	3.51
69.599	3065	3.065	0.0833	0.0021	69.52	4.73E-06	3.34E-02	1.75
78.861	2705.04	2.70504	0.0849	0.0016	70.82	4.80E-06	3.02E-02	1.34
91.005	2344.08	2.34408	0.087	0.0021	72.58	6.30E-06	3.42E-02	1.75
105.957	2013.29	2.01329	0.089	0.002	74.28	5.97E-06	2.78E-02	1.67
125.774	1696.08	1.69608	0.091	0.002	75.95	7.07E-06	2.79E-02	1.67
152.332	1400.37	1.40037	0.0935	0.0025	78.04	9.56E-06	3.11E-02	2.09
188.195	1133.51	1.13351	0.0964	0.0028	80.4	1.16E-05	3.07E-02	2.34

1	2	3	4	5	6	7	8	9
235.82	904.6	0.9046	0.0993	0.0029	82.86	1.38E-05	2.90E-02	2.42
297.421	717.24	0.71724	0.1022	0.0029	85.24	1.72E-05	2.87E-02	2.42
372.576	572.56	0.57256	0.105	0.0028	87.59	2.13E-05	2.83E-02	2.34
460.653	463.09	0.46309	0.1075	0.0026	89.71	2.60E-05	2.80E-02	2.17
561.515	379.9	0.3799	0.11	0.0024	91.76	3.05E-05	2.68E-02	2.00
675.16	315.96	0.31596	0.1119	0.0019	93.35	3.14E-05	2.30E-02	1.59
801.398	266.19	0.26619	0.1136	0.0018	94.82	3.80E-05	2.34E-02	1.50
937.525	227.54	0.22754	0.1149	0.0013	95.91	2.72E-05	1.42E-02	1.09
1120.011	190.46	0.19046	0.1158	0.0009	96.64	2.91E-05	1.30E-02	0.75
1370.933	155.6	0.1556	0.1172	0.0014	97.81	4.53E-05	1.63E-02	1.17
1658.168	128.65	0.12865	0.1183	0.0011	98.73	3.16E-05	9.27E-03	0.92
2020.769	105.56	0.10556	0.1188	0.0005	99.16	2.22E-05	5.44E-03	0.42
2504.408	85.18	0.08518	0.1193	0.0005	99.58	2.54E-05	4.98E-03	0.42
3106.577	68.67	0.06867	0.1197	0.0003	99.84	1.24E-05	1.93E-03	0.25
3835.079	55.62	0.05562	0.1198	0.0001	99.93	4.99E-06	6.16E-04	0.08
4716.453	45.23	0.04523	0.1198	0	99.93	0.00E+00	0.00E+00	0.00
5731.128	37.22	0.03722	0.1198	0	99.93	0.00E+00	0.00E+00	0.00
6807.617	31.34	0.03134	0.1198	0	99.94	8.55E-06	6.42E-04	0.00
7918.744	26.94	0.02694	0.1198	0.0001	100	9.14E-06	5.50E-04	0.08

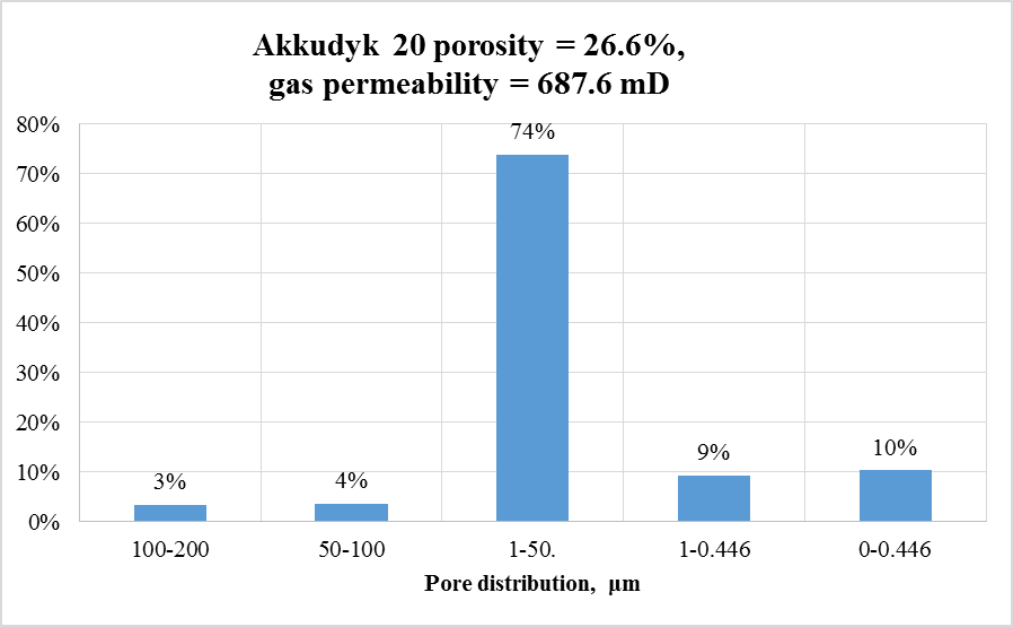

Figure B. 1 Pore size distribution sample Akkudyk 20

Table B. 2 Results of Mercury porosimeter of sample Akkudyk 19

Pressure [PSI]	Pore Diameter [nm]	Pore Diameter [μm]	Volume Intruded [cc/g]	Delta Volume [cc/g]	Volume Intruded %	Dv(d) [cc/(nm-g)]	dV/d(log [cc/g]	Pore size Distribution, %
1	2	3	4	5	6	7	8	9
67.88	3142.65	3.14	0.02	0.023	70.51	0.00	0.00	70.5
511.21	417.29	0.42	0.03	0.004	83.99	0.00	0.01	13.4
735.28	290.13	0.29	0.03	0.002	88.82	0.00	0.00	5.0
953.71	223.68	0.22	0.03	0.000	89.11	0.00	0.00	0.3
1259.73	169.34	0.17	0.03	0.000	89.31	0.00	0.00	0.3
1666.66	127.99	0.13	0.03	0.000	89.54	0.00	0.00	0.3
2194.42	97.21	0.10	0.03	0.000	90.08	0.00	0.00	0.6
2834.85	75.25	0.08	0.03	0.000	90.90	0.00	0.00	0.9
3609.17	59.11	0.06	0.03	0.000	90.96	0.00	0.00	0.0
4522.03	47.17	0.05	0.03	0.000	90.96	0.00	0.00	0.0
5520.15	38.64	0.04	0.03	0.000	91.37	0.00	0.00	0.3
6554.43	32.55	0.03	0.03	0.000	91.94	0.00	0.00	0.6
7609.63	28.03	0.03	0.03	0.000	92.79	0.00	0.00	0.9
8687.82	24.55	0.02	0.03	0.000	93.30	0.00	0.00	0.6
9807.23	21.75	0.02	0.03	0.000	93.68	0.00	0.00	0.3
10962.85	19.46	0.02	0.03	0.000	94.00	0.00	0.00	0.3
12154.67	17.55	0.02	0.03	0.000	94.30	0.00	0.00	0.3
13382.23	15.94	0.02	0.03	0.000	94.50	0.00	0.00	0.3
14644.95	14.57	0.01	0.03	0.000	94.61	0.00	0.00	0.0
15941.84	13.38	0.01	0.03	0.000	94.65	0.00	0.00	0.0
17274.11	12.35	0.01	0.03	0.000	95.03	0.00	0.00	0.3
18643.12	11.44	0.01	0.03	0.000	95.28	0.00	0.00	0.3
20048.70	10.64	0.01	0.03	0.000	95.36	0.00	0.00	0.0
21493.43	9.92	0.01	0.03	0.000	95.65	0.00	0.00	0.3
22977.04	9.28	0.01	0.03	0.000	95.74	0.00	0.00	0.0
24496.59	8.71	0.01	0.03	0.000	95.94	0.00	0.01	0.3
26051.99	8.19	0.01	0.03	0.000	96.87	0.00	0.01	0.9
27659.92	7.71	0.01	0.03	0.000	97.38	0.00	0.00	0.6
29387.48	8.26	0.01	0.03	0.000	97.49	0.00	0.00	0.0
31358.45	6.80	0.01	0.03	0.000	97.67	0.00	0.00	0.3
34206.80	6.24	0.01	0.03	0.000	98.39	0.00	0.01	0.6
37711.61	5.66	0.01	0.03	0.000	99.51	0.00	0.01	1.2
41413.02	5.15	0.01	0.03	0.000	100.00	0.00	0.00	0.6

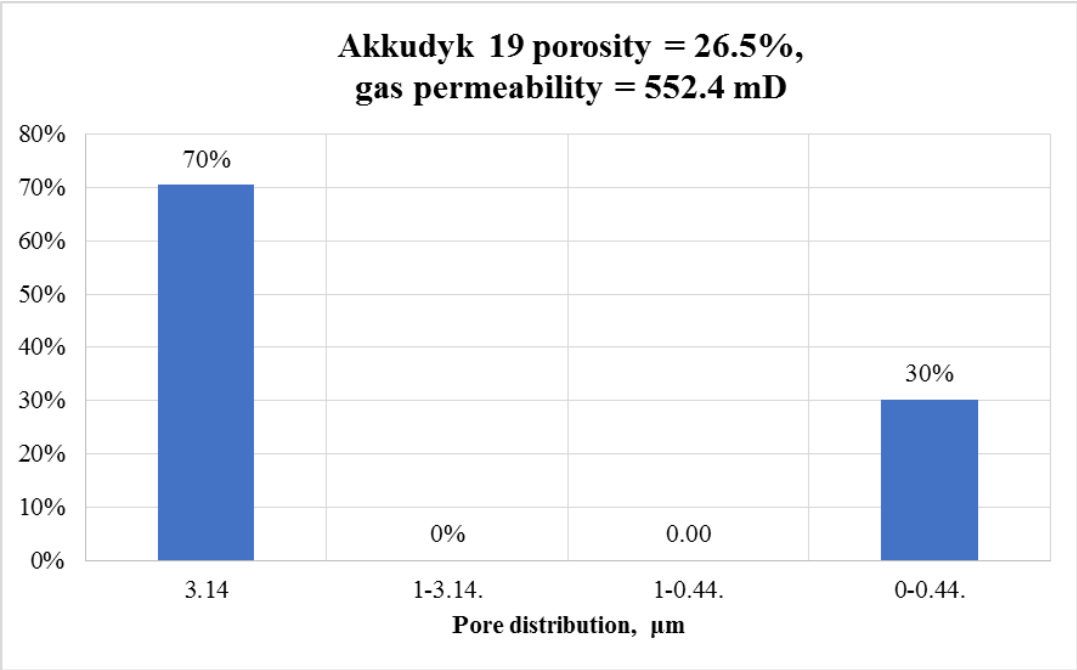

Figure B. 2Pore size distribution sample Akkudyk 19

Table B. 3Results of Mercury porosimeter of sample Botakhan

Pressure [PSI]	Pore Diameter [nm]	Pore Diameter [µm]	Volume Intruded [cc/g]	Delta Volume [cc/g]	Volume Intruded %	Dv(d) [cc/(nm-g)]	dV/d(log [cc/g]	Pore size Distribution, %
1	2	3	4	5	6	7	8	9
0.71	302142.4	302.14	0.00	0.0003	0.23	0.00	0.02	0.2%
2.18	97738.43	97.74	0.01	0.00580	5.06	0.00	0.02	4.8%
2.67	79810.74	79.81	0.01	0.00020	5.26	0.00	0.00	0.2%
3.13	68079.93	68.08	0.01	0.00030	5.49	0.00	0.01	0.2%
4.13	51663.56	51.66	0.01	0.00090	6.20	0.00	0.01	0.7%
4.78	44595.07	44.60	0.01	0.00050	6.58	0.00	0.01	0.4%
5.72	37326.16	37.33	0.01	0.00120	7.59	0.00	0.01	1.0%
6.50	32797.60	32.80	0.01	0.00040	7.96	0.00	0.01	0.3%
7.43	28707.70	28.71	0.01	0.00090	8.68	0.00	0.02	0.7%
8.48	25165.52	25.17	0.01	0.00070	9.24	0.00	0.01	0.6%
9.61	22200.18	22.20	0.01	0.00100	10.03	0.00	0.04	0.8%
10.83	19705.77	19.71	0.01	0.00280	12.32	0.00	0.08	2.3%
12.12	17596.75	17.60	0.02	0.00760	18.60	0.00	0.25	6.3%
13.27	16073.35	16.07	0.04	0.01470	30.80	0.00	0.42	12.2%
14.58	14632.23	14.63	0.05	0.01560	43.70	0.00	0.32	12.9%
15.95	13372.84	13.37	0.06	0.00930	51.39	0.00	0.19	7.7%
17.43	12242.64	12.24	0.07	0.00550	55.98	0.00	0.13	4.6%
19.01	11220.86	11.22	0.07	0.00420	59.47	0.00	0.10	3.5%
20.78	10264.86	10.26	0.08	0.00330	62.20	0.00	0.08	2.7%
22.54	9462.69	9.46	0.08	0.00220	64.00	0.00	0.06	1.8%
24.45	8724.38	8.72	0.08	0.00200	65.67	0.00	0.05	1.7%
26.35	8096.00	8.10	0.08	0.00160	66.97	0.00	0.05	1.3%
28.12	7586.97	7.59	0.08	0.00120	67.99	0.00	0.04	1.0%

1	2	3	4	5	6	7	8	9
30.10	7088.33	7.09	0.08	0.00120	69.00	0.00	0.05	1.0%
32.26	6612.91	6.61	0.08	0.00150	70.25	0.00	0.03	1.2%
34.79	6131.88	6.13	0.09	0.00060	70.77	0.00	0.02	0.5%
37.57	5677.96	5.68	0.09	0.00090	71.49	0.00	0.03	0.7%
40.41	5279.59	5.28	0.09	0.00130	72.57	0.00	0.04	1.1%
43.04	4956.27	4.96	0.09	0.00060	73.10	0.00	0.03	0.5%
45.74	4663.96	4.66	0.09	0.00080	73.74	0.00	0.02	0.7%
49.16	4339.31	4.34	0.09	0.00040	74.08	0.00	0.01	0.3%
56.03	3807.39	3.81	0.09	0.00070	74.67	0.00	0.02	0.6%
67.27	3171.00	3.17	0.09	0.00150	75.93	0.00	0.02	1.2%
80.09	2663.56	2.66	0.09	0.00200	77.62	0.00	0.03	1.7%
92.55	2305.02	2.31	0.09	0.00120	78.64	0.00	0.01	1.0%
111.07	1920.57	1.92	0.10	0.00110	79.55	0.00	0.02	0.9%
137.47	1551.75	1.55	0.10	0.00190	81.13	0.00	0.02	1.6%
169.36	1259.55	1.26	0.10	0.00150	82.39	0.00	0.01	1.2%
214.95	992.44	0.99	0.10	0.00150	83.61	0.00	0.01	1.2%
274.24	777.86	0.78	0.10	0.00170	85.00	0.00	0.02	1.4%
345.33	617.73	0.62	0.10	0.00180	86.49	0.00	0.02	1.5%
430.98	494.97	0.49	0.11	0.00140	87.66	0.00	0.01	1.2%
536.07	397.94	0.40	0.11	0.00130	88.72	0.00	0.02	1.1%
652.88	326.74	0.33	0.11	0.00140	89.92	0.00	0.02	1.2%
778.69	273.95	0.27	0.11	0.00120	90.94	0.00	0.02	1.0%
923.20	231.07	0.23	0.11	0.00110	91.87	0.00	0.01	0.9%
1104.99	193.05	0.19	0.11	0.00070	92.44	0.00	0.01	0.6%
1362.58	156.56	0.16	0.11	0.00110	93.33	0.00	0.01	0.9%
1691.52	126.11	0.13	0.11	0.00080	94.00	0.00	0.01	0.7%
2113.47	100.93	0.10	0.11	0.00100	94.80	0.00	0.01	0.8%
2598.52	82.09	0.08	0.12	0.00090	95.57	0.00	0.01	0.7%
3159.99	67.51	0.07	0.12	0.00060	96.07	0.00	0.01	0.5%
3841.38	55.53	0.06	0.12	0.00030	96.33	0.00	0.00	0.2%
4671.94	45.66	0.05	0.12	0.00030	96.56	0.00	0.00	0.2%
5647.08	37.78	0.04	0.12	0.00050	97.00	0.00	0.01	0.4%
6715.65	31.76	0.03	0.12	0.00070	97.57	0.00	0.01	0.6%
7823.72	27.27	0.03	0.12	0.00050	97.95	0.00	0.01	0.4%
8958.35	23.81	0.02	0.12	0.00030	98.22	0.00	0.01	0.2%
10116.73	21.09	0.02	0.12	0.00020	98.41	0.00	0.00	0.2%
11322.41	18.84	0.02	0.12	0.00030	98.66	0.00	0.01	0.2%
12567.49	16.97	0.02	0.12	0.00050	99.10	0.00	0.01	0.4%
13850.64	15.40	0.02	0.12	0.00030	99.32	0.00	0.01	0.2%
15172.64	14.06	0.01	0.12	0.00020	99.46	0.00	0.00	0.2%
16533.50	12.90	0.01	0.12	0.00010	99.52	0.00	0.00	0.1%
17936.06	11.89	0.01	0.12	0.00000	99.53	0.00	0.00	0.0%
19379.02	11.01	0.01	0.12	0.00000	99.53	0.00	0.00	0.0%
20862.57	10.23	0.01	0.12	0.00010	99.58	0.00	0.00	0.1%
22388.02	9.23	0.01	0.12	0.00000	99.60	0.00	0.00	0.0%
23954.36	8.91	0.01	0.12	0.00030	99.84	0.00	0.01	0.2%
25560.15	8.35	0.01	0.12	0.00020	100.00	0.00	0.00	0.2%

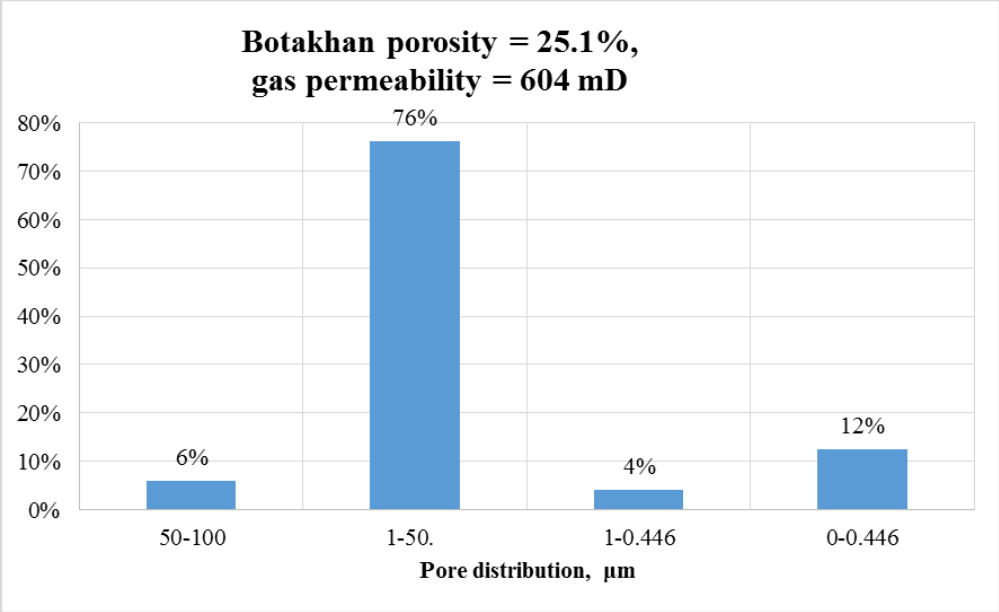

Figure B. 3 Pore size distribution sample Botakhan

Table B. 4 Results of Mercury porosimeter of sample Akshabulak 45

Pressure [PSI]	Pore Diameter [nm]	Pore Diameter [µm]	Volume Intruded [cc/g]	Delta Volume [cc/g]	Volume Intruded %	Dv(d) [cc/(nm-g)]	dV/d(log [cc/g]	Pore size Distribution, %
1	2	3	4	5	6	7	8	9
0.829	257290.9	257.2909	0	0	0	1.36E-08	8.49E-03	0.00
1.291	165234.4	165.2344	0.0016	0.0016	1.02	2.16E-08	8.34E-03	1.04
1.68	126972.5	126.9725	0.0026	0.001	1.71	2.11E-08	6.07E-03	0.65
2.196	97156.25	97.15625	0.0031	0.0005	2.02	1.96E-08	4.53E-03	0.33
3.082	69210.42	69.21042	0.0039	0.0008	2.52	9.24E-08	1.53E-02	0.52
3.591	59409.39	59.40939	0.0056	0.0017	3.63	1.60E-07	2.16E-02	1.11
4.362	48909.03	48.90903	0.0061	0.0006	4	0.00E+00	0.00E+00	0.39
5.12	41661.75	41.66175	0.0065	0.0004	4.26	1.33E-07	1.32E-02	0.26
5.985	35642.03	35.64203	0.0075	0.001	4.91	1.17E-07	9.40E-03	0.65
6.958	30658.08	30.65808	0.0078	0.0003	5.08	2.57E-08	1.78E-03	0.20
7.844	27195.88	27.19588	0.0078	0	5.09	2.89E-08	1.90E-03	0.00
8.785	24283.42	24.28342	0.0081	0.0003	5.27	1.18E-07	6.64E-03	0.20
10.047	21233.26	21.23326	0.0084	0.0004	5.51	2.01E-07	1.00E-02	0.26
11.381	18744.54	18.74454	0.0092	0.0008	6.01	3.75E-07	1.64E-02	0.52
12.556	16989.96	16.98996	0.0103	0.001	6.7	1.05E-06	4.16E-02	0.65
13.713	15556.29	15.55629	0.0132	0.0029	8.59	3.31E-06	1.20E-01	1.89
15.025	14197.63	14.19763	0.0201	0.007	13.14	7.37E-06	2.43E-01	4.57
16.571	12873.58	12.87358	0.0355	0.0154	23.18	1.49E-05	4.47E-01	10.05
18.301	11656.05	11.65605	0.0565	0.0209	36.85	1.58E-05	4.24E-01	13.64
19.97	10682.22	10.68222	0.0694	0.013	45.31	1.18E-05	2.91E-01	8.49
21.72	9821.3	9.8213	0.0781	0.0087	50.98	9.24E-06	2.09E-01	5.68
23.531	9065.76	9.06576	0.0843	0.0062	55.02	7.59E-06	1.59E-01	4.05
25.306	8429.86	8.42986	0.0887	0.0044	57.9	6.45E-06	1.25E-01	2.87
27.031	7891.74	7.89174	0.092	0.0033	60.06	6.02E-06	1.10E-01	2.15
28.639	7448.66	7.44866	0.0947	0.0027	61.82	6.19E-06	1.07E-01	1.76
30.585	6974.78	6.97478	0.0976	0.0029	63.69	5.73E-06	9.21E-02	1.89
32.567	6550.35	6.55035	0.0997	0.0021	65.08	4.90E-06	7.41E-02	1.37
35.181	6063.6	6.0636	0.1022	0.0025	66.69	5.10E-06	7.14E-02	1.63
38.007	5612.69	5.61269	0.1044	0.0022	68.15	4.49E-06	5.81E-02	1.44

1	2	3	4	5	6	7	8	9
40.711	5239.9	5.2399	0.1059	0.0015	69.13	3.99E-06	4.83E-02	0.98
43.217	4936.05	4.93605	0.1072	0.0012	69.92	4.19E-06	4.77E-02	0.78
46.226	4614.75	4.61475	0.1085	0.0013	70.8	4.26E-06	4.54E-02	0.85
51.416	4148.91	4.14891	0.1109	0.0024	72.34	5.86E-06	5.73E-02	1.57
63.487	3360.09	3.36009	0.1172	0.0063	76.46	9.11E-06	7.05E-02	4.11
72.778	2931.14	2.93114	0.1207	0.0035	78.77	6.39E-06	4.29E-02	2.28
82.675	2580.24	2.58024	0.1222	0.0015	79.76	3.73E-06	2.22E-02	0.98
98.231	2171.64	2.17164	0.1239	0.0016	80.84	5.02E-06	2.56E-02	1.04
118.89	1794.28	1.79428	0.1266	0.0027	82.59	8.17E-06	3.39E-02	1.76
142.13	1500.89	1.50089	0.1288	0.0022	84.01	6.26E-06	2.16E-02	1.44
174.924	1219.51	1.21951	0.1304	0.0016	85.08	6.97E-06	1.99E-02	1.04
220.463	967.61	0.96761	0.1326	0.0022	86.52	9.28E-06	2.07E-02	1.44
277.653	768.3	0.7683	0.1344	0.0018	87.71	9.21E-06	1.64E-02	1.17
354.531	601.7	0.6017	0.1359	0.0015	88.69	9.62E-06	1.35E-02	0.98
457.081	466.71	0.46671	0.1374	0.0014	89.63	1.04E-05	1.12E-02	0.91
598.957	356.16	0.35616	0.1383	0.0009	90.24	8.69E-06	7.23E-03	0.59
814.613	261.87	0.26187	0.1393	0.001	90.9	1.18E-05	7.09E-03	0.65
1117.066	190.97	0.19097	0.1401	0.0008	91.42	1.23E-05	5.51E-03	0.52
1542.622	138.29	0.13829	0.141	0.0009	91.99	2.06E-05	6.62E-03	0.59
2103.974	101.39	0.10139	0.1419	0.0009	92.58	2.94E-05	6.92E-03	0.59
2787.602	76.53	0.07653	0.1428	0.0009	93.16	5.11E-05	9.26E-03	0.59
3573.043	59.7	0.0597	0.1442	0.0014	94.1	1.15E-04	1.60E-02	0.91
4422.335	48.24	0.04824	0.1458	0.0016	95.13	1.62E-04	1.82E-02	1.04
5337.242	39.97	0.03997	0.1474	0.0016	96.16	1.96E-04	1.81E-02	1.04
6323.917	33.73	0.03373	0.1485	0.0012	96.93	1.91E-04	1.49E-02	0.78
7404.795	28.81	0.02881	0.1495	0.001	97.55	2.01E-04	1.34E-02	0.65
8526.123	25.02	0.02502	0.1502	0.0008	98.04	1.64E-04	9.39E-03	0.52
9687.493	22.02	0.02202	0.1506	0.0003	98.26	1.17E-04	5.97E-03	0.20
10892.36	19.58	0.01958	0.1509	0.0003	98.49	1.29E-04	5.81E-03	0.20
12134.64	17.58	0.01758	0.1511	0.0002	98.62	9.37E-05	3.81E-03	0.13
13417.86	15.9	0.0159	0.1513	0.0001	98.71	5.74E-05	2.09E-03	0.07
14738.59	14.47	0.01447	0.1513	0.0001	98.75	5.45E-05	1.83E-03	0.07
16097.46	13.25	0.01325	0.1514	0.0001	98.8	1.20E-04	3.73E-03	0.07
17497.8	12.19	0.01219	0.1517	0.0003	98.97	3.03E-04	8.54E-03	0.20
18939.12	11.26	0.01126	0.1519	0.0002	99.11	1.51E-04	3.90E-03	0.13
20421.01	10.45	0.01045	0.152	0.0001	99.17	6.21E-05	1.48E-03	0.07
21944.2	9.72	0.00972	0.152	0	99.18	0.00E+00	0.00E+00	0.00
23508.42	9.07	0.00907	0.152	0	99.18	0.00E+00	0.00E+00	0.00
25112.65	8.49	0.00849	0.152	0	99.18	0.00E+00	0.00E+00	0.00
26758.19	7.97	0.00797	0.152	0	99.18	2.55E-06	4.84E-05	0.00
28443.02	7.5	0.0075	0.152	0.0001	99.21	4.55E-04	7.98E-03	0.07
30149.45	7.08	0.00708	0.1524	0.0004	99.44	6.36E-04	1.03E-02	0.26
31960.42	6.67	0.00667	0.1525	0.0001	99.49	5.03E-05	7.60E-04	0.07
33934.07	6.29	0.00629	0.1525	0	99.49	0.00E+00	0.00E+00	0.00
36616.51	5.83	0.00583	0.1525	0	99.49	8.10E-05	1.13E-03	0.00
40376.98	5.28	0.00528	0.1527	0.0002	99.62	6.24E-04	7.68E-03	0.13
44431.12	4.8	0.0048	0.153	0.0004	99.86	6.17E-04	6.80E-03	0.26
48647.82	4.39	0.00439	0.1532	0.0002	99.97	4.29E-04	4.31E-03	0.13

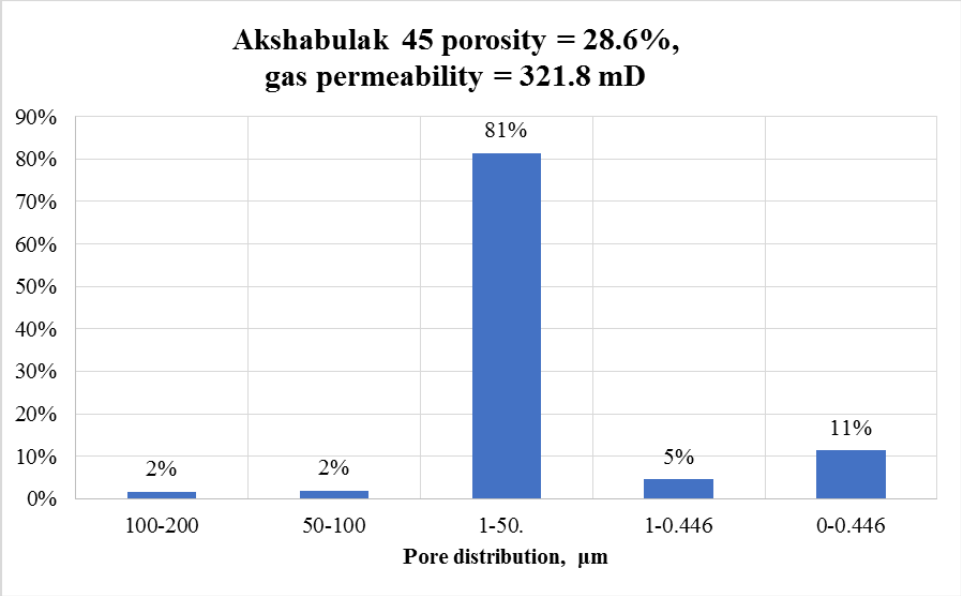

Figure B. 4Pore size distribution sample Akshabulak 45

Table B. 5Results of Mercury porosimeter of sample Akshabulak 206

Pressure [PSI]	Pore Diameter [nm]	Pore Diameter [µm]	Volume Intruded [cc/g]	Delta Volume [cc/g]	Volume Intruded %	Dv(d) [cc/(nm-g)]	dV/d(log [cc/g]	Pore size Distribution, %
1	2	3	4	5	6	7	8	9
0.818	260690.13	260.69013	0	0	0.00	4.81E-09	3.29E-03	0%
1.64	130068.63	130.06863	0.0018	0.0018	1.91	2.15E-08	6.48E-03	1.92%
2.464	86566.11	86.56611	0.003	0.0012	3.17	2.79E-08	5.53E-03	1.28%
3.166	67382.48	67.38248	0.0036	0.0007	3.88	5.21E-08	8.29E-03	0.75%
3.924	54366.09	54.36609	0.0045	0.0009	4.83	8.45E-08	1.07E-02	0.96%
4.746	44948.13	44.94813	0.0057	0.0011	6.05	1.70E-07	1.79E-02	1.17%
5.589	38171.43	38.17143	0.0075	0.0018	8.00	4.19E-07	3.76E-02	1.92%
6.438	33136.93	33.13693	0.0108	0.0033	11.49	7.58E-07	5.81E-02	3.52%
7.406	28803.53	28.80353	0.0144	0.0037	15.40	1.07E-06	7.23E-02	3.95%
8.584	24850.58	24.85058	0.0198	0.0053	21.06	1.34E-06	7.67E-02	5.66%
9.883	21584.41	21.58441	0.0239	0.0042	25.53	1.31E-06	6.53E-02	4.48%
11.23	18996.29	18.99629	0.027	0.0031	28.84	1.04E-06	4.55E-02	3.31%
12.667	16840.69	16.84069	0.029	0.002	30.96	9.62E-07	3.74E-02	2.13%
14.118	15109.63	15.10963	0.0306	0.0016	32.63	9.75E-07	3.41E-02	1.71%
15.513	13750.88	13.75088	0.0322	0.0016	34.31	1.09E-06	3.46E-02	1.71%
16.9	12622.72	12.62272	0.0333	0.0012	35.55	1.02E-06	2.99E-02	1.28%
18.652	11436.7	11.4367	0.0346	0.0013	36.94	1.31E-06	3.47E-02	1.39%
20.446	10433.38	10.43338	0.0363	0.0017	38.75	2.13E-06	5.15E-02	1.81%
22.168	9622.85	9.62285	0.0382	0.0019	40.76	1.81E-06	3.99E-02	2.03%
23.892	8928.78	8.92878	0.0392	0.001	41.79	1.56E-06	3.23E-02	1.07%
25.681	8306.62	8.30662	0.0402	0.001	42.9	1.61E-06	3.08E-02	1.07%
27.502	7756.65	7.75665	0.041	0.0008	43.73	1.20E-06	2.14E-02	0.85%
29.318	7276.05	7.27605	0.0416	0.0006	44.32	1.45E-06	2.44E-02	0.64%
31.258	6824.48	6.82448	0.0424	0.0008	45.22	1.90E-06	3.00E-02	0.85%
33.665	6336.62	6.33662	0.0433	0.0009	46.13	1.86E-06	2.72E-02	0.96%
36.429	5855.86	5.85586	0.0443	0.001	47.2	2.17E-06	2.94E-02	1.07%
39.078	5458.86	5.45886	0.0451	0.0009	48.11	2.02E-06	2.54E-02	0.96%
41.688	5117.15	5.11715	0.0458	0.0007	48.85	2.16E-06	2.55E-02	0.75%
44.464	4797.63	4.79763	0.0466	0.0007	49.64	2.54E-06	2.81E-02	0.75%
47.672	4474.82	4.47482	0.0473	0.0007	50.42	2.10E-06	2.17E-02	0.75%

1	2	3	4	5	6	7	8	9
52.747	4044.26	4.04426	0.0482	0.0009	51.39	2.08E-06	1.96E-02	0.96%
62.884	3392.33	3.39233	0.0498	0.0016	53.13	3.14E-06	2.49E-02	1.71%
74.597	2859.68	2.85968	0.0521	0.0022	55.53	4.88E-06	3.23E-02	2.35%
86.094	2477.79	2.47779	0.0539	0.0018	57.47	4.68E-06	2.69E-02	1.92%
100.707	2118.26	2.11826	0.0558	0.0019	59.49	5.72E-06	2.81E-02	2.03%
119.396	1786.68	1.78668	0.0579	0.0021	61.69	7.02E-06	2.92E-02	2.24%
143.955	1481.87	1.48187	0.0603	0.0025	64.32	8.72E-06	3.00E-02	2.67%
176.567	1208.17	1.20817	0.063	0.0027	67.15	1.09E-05	3.07E-02	2.88%
220.361	968.06	0.96806	0.0659	0.003	70.31	1.36E-05	3.07E-02	3.20%
277.58	768.51	0.76851	0.069	0.003	73.56	1.73E-05	3.09E-02	3.20%
348.852	611.5	0.6115	0.0723	0.0033	77.05	2.45E-05	3.49E-02	3.52%
433.309	492.31	0.49231	0.0756	0.0034	80.63	3.14E-05	3.59E-02	3.63%
529.679	402.74	0.40274	0.0787	0.0031	83.95	3.62E-05	3.37E-02	3.31%
637.817	334.46	0.33446	0.0812	0.0025	86.61	3.54E-05	2.73E-02	2.67%
761.325	280.2	0.2802	0.083	0.0018	88.51	3.42E-05	2.22E-02	1.92%
898.342	237.46	0.23746	0.0845	0.0015	90.15	3.64E-05	2.00E-02	1.60%
1052.767	202.63	0.20263	0.086	0.0015	91.71	5.19E-05	2.45E-02	1.60%
1215.234	175.54	0.17554	0.0876	0.0016	93.4	5.04E-05	2.03E-02	1.71%
1395.551	152.86	0.15286	0.0883	0.0007	94.19	2.95E-05	1.05E-02	0.75%
1636.917	130.32	0.13032	0.0892	0.0008	95.06	4.31E-05	1.30E-02	0.85%
1950.859	109.35	0.10935	0.0901	0.001	96.11	4.29E-05	1.08E-02	1.07%
2334.746	91.37	0.09137	0.0907	0.0006	96.74	2.44E-05	5.08E-03	0.64%
2816.027	75.75	0.07575	0.0909	0.0002	96.94	8.19E-06	1.43E-03	0.21%
3414.881	62.47	0.06247	0.0911	0.0002	97.12	1.74E-05	2.53E-03	0.21%
4119.473	51.78	0.05178	0.0913	0.0002	97.31	1.58E-05	1.90E-03	0.21%
4955.43	43.05	0.04305	0.0914	0.0001	97.45	9.40E-06	8.97E-04	0.11%
5926.138	36	0.036	0.0914	0	97.46	4.94E-06	4.41E-04	0.00%
7005.984	30.45	0.03045	0.0915	0.0001	97.6	4.34E-05	3.08E-03	0.11%
8126.076	26.25	0.02625	0.0917	0.0002	97.82	5.73E-05	3.52E-03	0.21%
9269.087	23.01	0.02301	0.092	0.0003	98.09	6.17E-05	3.23E-03	0.32%
10459.076	20.4	0.0204	0.0921	0.0001	98.16	2.36E-05	1.13E-03	0.11%
11687.966	18.25	0.01825	0.0922	0.0001	98.29	9.71E-05	4.12E-03	0.11%
12955.422	16.47	0.01647	0.0924	0.0002	98.49	5.57E-05	2.08E-03	0.21%
14262.372	14.96	0.01496	0.0924	0	98.52	3.93E-05	1.39E-03	0.00%
15606.601	13.67	0.01367	0.0926	0.0002	98.68	1.82E-04	5.78E-03	0.21%
16990.564	12.56	0.01256	0.0927	0.0002	98.89	1.48E-04	4.27E-03	0.21%
18416.477	11.58	0.01158	0.0929	0.0001	99.01	1.32E-04	3.54E-03	0.11%
19881.631	10.73	0.01073	0.093	0.0002	99.18	1.45E-04	3.55E-03	0.21%
21388.773	9.97	0.00997	0.0931	0.0001	99.24	6.98E-05	1.61E-03	0.11%
22936.35	9.30	0.0093	0.0931	0	99.28	4.60E-05	9.82E-04	0.00%
24523.342	8.70	0.0087	0.0931	0	99.31	1.91E-05	3.77E-04	0.00%
26152.555	8.16	0.00816	0.0932	0	99.32	1.06E-04	2.02E-03	0.00%
27861.605	7.66	0.00766	0.0933	0.0001	99.46	2.67E-04	4.71E-03	0.11%
29666.225	7.19	0.00719	0.0933	0.0001	99.52	2.71E-05	4.40E-04	0.11%
31418.43	6.79	0.00679	0.0933	0	99.52	0.00E+00	0.00E+00	0.00%
33195.992	6.43	0.00643	0.0933	0	99.52	1.48E-04	2.23E-03	0.00%
35171.09	6.07	0.00607	0.0935	0.0001	99.66	3.05E-04	4.24E-03	0.11%
38294.555	5.57	0.00557	0.0935	0	99.7	1.66E-05	2.15E-04	0.00%
42230.719	5.05	0.00505	0.0936	0.0001	99.75	2.53E-04	3.00E-03	0.11%
46355.223	4.60	0.0046	0.0937	0.0002	99.94	3.46E-04	3.65E-03	0.21%

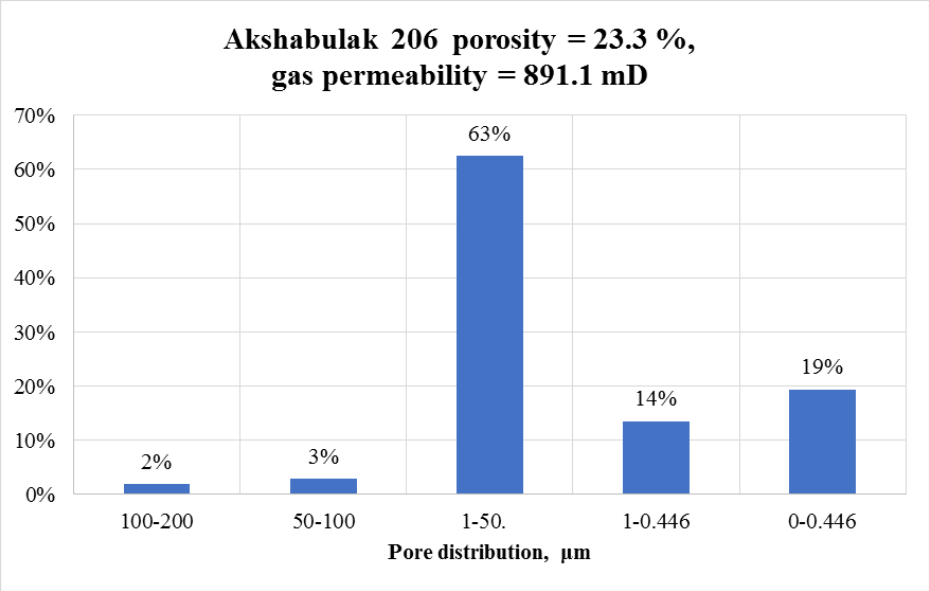

Figure B. 5Pore size distribution sample Akshabulak 206

Table B. 6 Results of Mercury porosimeter of sample Akshabulak 500

Pressure [PSI]	Pore Diameter [nm]	Pore Diameter [µm]	Volume Intruded [cc/g]	Delta Volume [cc/g]	Volume Intruded %	Dv(d) [cc/(nm-g)]	dV/d(log [cc/g]	Pore size Distribution, %
1	2	3	4	5	6	7	8	9
0.818	340280.2	340.2802	0.0000	0.0000	0.00	4.81E-09	3.29E-03	0.00
1.64	239065.5	239.0655	0.0016	0.0016	1.91	2.15E-08	6.48E-03	1.52
2.464	182181.3	182.1813	0.0029	0.0013	3.17	2.79E-08	5.53E-03	1.28
3.166	153078.5	153.0785	0.0037	0.0008	3.88	5.21E-08	8.29E-03	0.75
3.924	117888.6	117.8886	0.0047	0.0010	4.83	8.45E-08	1.07E-02	0.96
4.746	99574.4	99.5744	0.0062	0.0016	6.05	1.70E-07	1.79E-02	1.50
5.589	73079.42	73.07942	0.0082	0.0020	8.00	4.19E-07	3.76E-02	1.92
6.438	62806.63	62.80663	0.0109	0.0026	11.49	7.58E-07	5.81E-02	2.52
7.406	52863.82	52.86382	0.0145	0.0037	15.40	1.07E-06	7.23E-02	3.55
8.584	44432.6	44.4326	0.0183	0.0038	21.06	1.34E-06	7.67E-02	3.66
9.883	38471.52	38.47152	0.0217	0.0034	25.53	1.31E-06	6.53E-02	3.28
11.23	33865.92	33.86592	0.0252	0.0034	28.84	1.04E-06	4.55E-02	3.31
12.667	29550.01	29.55001	0.0274	0.0022	30.96	9.62E-07	3.74E-02	2.14
14.118	26648.9	26.6489	0.0292	0.0018	32.63	9.75E-07	3.41E-02	1.71
15.513	23489.4	23.4894	0.0310	0.0018	34.31	1.09E-06	3.46E-02	1.71
16.9	21149.8	21.1498	0.0323	0.0013	35.55	1.02E-06	2.99E-02	1.28
18.652	18818.53	18.81853	0.0337	0.0014	36.94	1.31E-06	3.47E-02	1.39
20.446	16890.39	16.89039	0.0356	0.0019	38.75	2.13E-06	5.15E-02	1.82
22.168	15435.46	15.43546	0.0377	0.0021	40.76	1.81E-06	3.99E-02	2.03
23.892	14177.14	14.17714	0.0388	0.0011	41.79	1.56E-06	3.23E-02	1.07
25.681	13004.6	13.0046	0.0400	0.0011	42.9	1.61E-06	3.08E-02	1.07
27.502	11976.5	11.9765	0.0408	0.0009	43.73	1.20E-06	2.14E-02	0.85
29.318	11062.32	11.06232	0.0415	0.0007	44.32	1.45E-06	2.44E-02	0.64
31.258	10284.35	10.28435	0.0424	0.0009	45.22	1.90E-06	3.00E-02	0.85
33.665	9674.314	9.674314	0.0434	0.0010	46.13	1.86E-06	2.72E-02	0.96
36.429	9046.258	9.046258	0.0445	0.0011	47.2	2.17E-06	2.94E-02	1.07
39.078	8506.745	8.506745	0.0455	0.0010	48.11	2.02E-06	2.54E-02	0.96
41.688	7928.765	7.928765	0.0463	0.0008	48.85	2.16E-06	2.55E-02	0.75

1	2	3	4	5	6	7	8	9
44.464	7326.202	7.326202	0.0470	0.0008	49.64	2.54E-06	2.81E-02	0.75
47.672	6810.05	6.81005	0.0478	0.0008	50.42	2.10E-06	2.17E-02	0.75
52.747	6403.865	6.403865	0.0488	0.0010	51.39	2.08E-06	1.96E-02	0.96
62.884	6018.87	6.01887	0.0506	0.0018	53.13	3.14E-06	2.49E-02	1.71
74.597	5366.608	5.366608	0.0530	0.0024	55.53	4.88E-06	3.23E-02	2.35
86.094	4485.494	4.485494	0.0550	0.0020	57.47	4.68E-06	2.69E-02	1.92
100.707	3984.5	3.9845	0.0571	0.0021	59.49	5.72E-06	2.81E-02	2.03
119.396	3516.552	3.516552	0.0595	0.0023	61.69	7.02E-06	2.92E-02	2.24
143.955	3047.304	3.047304	0.0622	0.0028	64.32	8.72E-06	3.00E-02	2.67
176.567	2617.277	2.617277	0.0652	0.0030	67.15	1.09E-05	3.07E-02	2.88
220.361	2204.904	2.204904	0.0686	0.0033	70.31	1.36E-05	3.07E-02	3.20
277.58	1820.481	1.820481	0.0719	0.0033	73.56	1.73E-05	3.09E-02	3.20
348.852	1473.563	1.473563	0.0755	0.0037	77.05	2.45E-05	3.49E-02	3.52
433.309	1175.98	1.17598	0.0793	0.0038	80.63	3.14E-05	3.59E-02	3.63
529.679	932.412	0.932412	0.0827	0.0034	83.95	3.62E-05	3.37E-02	3.31
637.817	744.328	0.744328	0.0843	0.0015	86.61	3.54E-05	2.73E-02	1.47
761.325	602.017	0.602017	0.0856	0.0014	88.51	3.42E-05	2.22E-02	1.32
898.342	493.87	0.49387	0.0873	0.0017	90.15	3.64E-05	2.00E-02	1.60
1052.767	410.748	0.410748	0.0890	0.0017	91.71	5.19E-05	2.45E-02	1.60
1215.234	346.047	0.346047	0.0907	0.0018	93.4	5.04E-05	2.03E-02	1.71
1395.551	295.802	0.295802	0.0920	0.0012	94.19	2.95E-05	1.05E-02	1.17
1636.917	247.598	0.247598	0.0931	0.0011	95.06	4.31E-05	1.30E-02	1.07
1950.859	202.28	0.20228	0.0937	0.0007	96.11	4.29E-05	1.08E-02	0.64
2334.746	167.245	0.167245	0.0946	0.0009	96.74	2.44E-05	5.08E-03	0.85
2816.027	137.228	0.137228	0.0954	0.0008	96.94	8.19E-06	1.43E-03	0.75
3414.881	110.734	0.110734	0.0959	0.0006	97.12	1.74E-05	2.53E-03	0.53
4119.473	89.271	0.089271	0.0969	0.0010	97.31	1.58E-05	1.90E-03	0.96
4955.43	72.306	0.072306	0.0979	0.0010	97.45	9.40E-06	8.97E-04	0.96
5926.138	58.799	0.058799	0.0988	0.0009	97.46	4.94E-06	4.41E-04	0.85
7005.984	48.386	0.048386	0.0994	0.0006	97.6	4.34E-05	3.08E-03	0.53
8126.076	40.742	0.040742	0.1002	0.0008	97.82	5.73E-05	3.52E-03	0.75
9269.087	35.022	0.035022	0.1002	0.0000	98.09	6.17E-05	3.23E-03	0.03
10459.08	32.526	0.032526	0.1007	0.0005	98.16	2.36E-05	1.13E-03	0.48
11687.97	28.626	0.028626	0.1009	0.0002	98.29	9.71E-05	4.12E-03	0.24
12955.42	25.454	0.025454	0.1017	0.0007	98.49	5.57E-05	2.08E-03	0.71
14262.37	22.854	0.022854	0.1019	0.0002	98.52	3.93E-05	1.39E-03	0.24
15606.6	20.67	0.02067	0.1021	0.0001	98.68	1.82E-04	5.78E-03	0.14
16990.56	18.811	0.018811	0.1022	0.0001	98.89	1.48E-04	4.27E-03	0.14
18416.48	17.225	0.017225	0.1029	0.0007	99.01	1.32E-04	3.54E-03	0.67
19881.63	15.847	0.015847	0.1039	0.0010	99.18	1.45E-04	3.55E-03	0.99
21388.77	14.638	0.014638	0.1039	0.0000	99.24	6.98E-05	1.61E-03	0.03

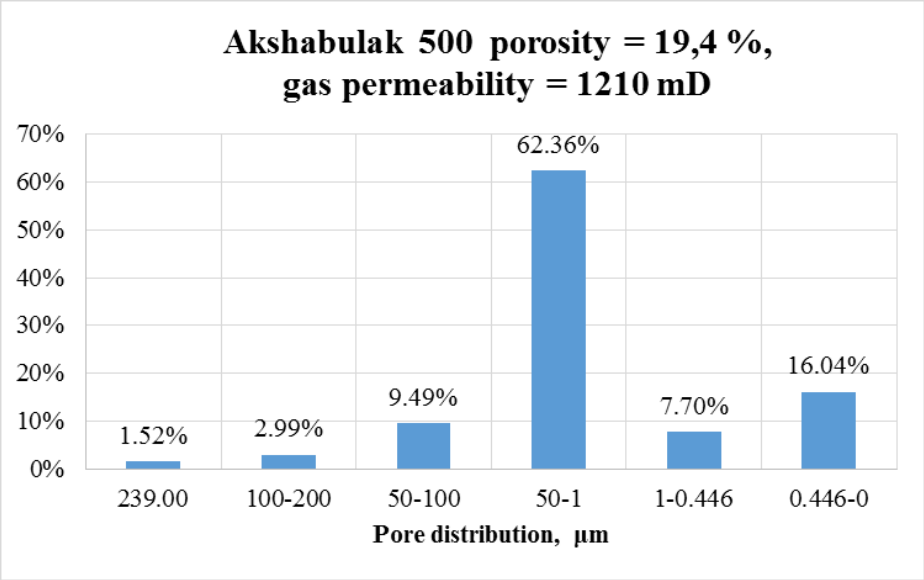

Figure B. 6Pore size distribution sample Akshabulak 500

Appendix C

Appendix C presents the raw and calculated data of 3 polymer powder.

Table C 1 Mass fraction of the main substance

	FP 3630	FP 5115	FP 5205
Mass of polymer before drying, g	2.558	2.183	2.24
Mass of polymer after drying, g	2.309	1.966	2.024
Mass fraction of the main substance,%	90.27%	90.06%	90.36%

Table C 2 Hydrolysis degree

	FP 3630	FP 5115	FP 5205
Mass of polymer, g	0.33	0.33	0.33
Volume of NaOH solution for working sample titration, ml	8.15	4.5	5.6
Volume of NaOH solution for working blank titration, ml	1.2	1.2	1.2
molar concentration of NaOH, mol/l	0.05	0.05	0.05
Polymer mass, g	0.106	0.107	0.107
Hydrolysis degree, %	25%	11%	15%

Table C 3 Intrinsic viscosity of sample FP3630

	Polymer drainage time , sec. (t)	Average polymer drainage time , sec. (t avr)	Relative viscosity ηrel=tavr/ t_{0*}	Specific viscosity, ηsp = ηrel -1	Mass concentration of polymer solution, g/dL Ci	Reduced viscosity, dL/g ηsp/ Ci
C1	228.07	228.1	1.950	0.950	0.045	21.105
	228.05					
	228.03					
C2	206.6	206.6	1.767	0.767	0.037	20.955
	206.7					
	206.6					
C3	184.06	184.4	1.576	0.576	0.028	20.498
	184.53					
	184.595					
C4	163.62	163.6	1.398	0.398	0.020	20.258
	163.56					
	163.5					
C5	143.12	143.1	1.223	0.223	0.011	19.835
	143.01					
	143.065					

*t_0=116.965

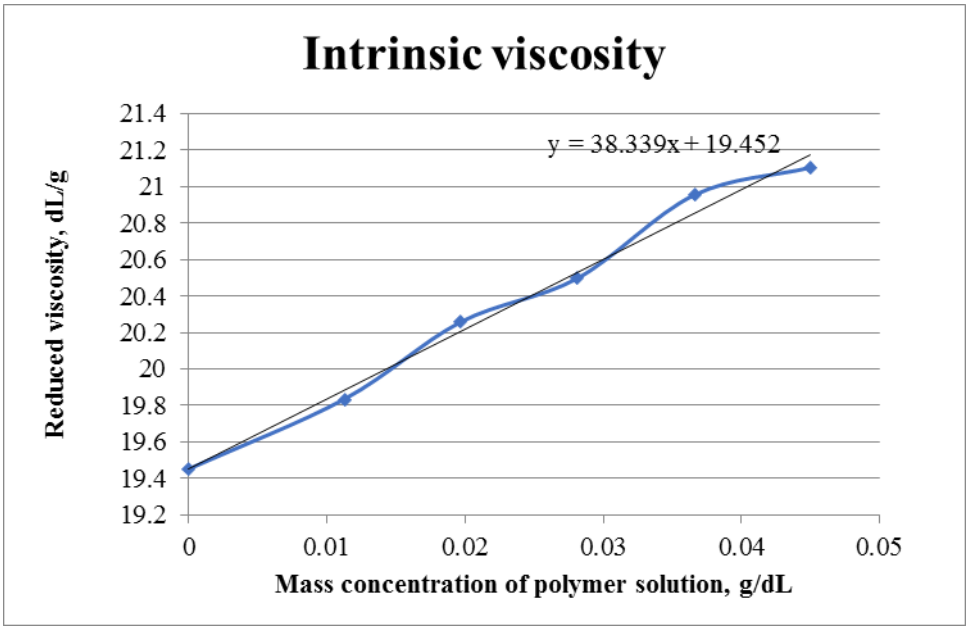

Figure C 1 Intrinsic viscosity of sample FP3630

Table C 4 Intrinsic viscosity of sample FP5115

	Polymer drainage time , sec. (t)	Average polymer drainage time , sec. (t avr)	Relative viscosity ηrel=tavr/ t_{0*}	Specific viscosity, ηsp = ηrel -1	Mass concentration of polymer solution, g/dL Ci	Reduced viscosity, dL/g ηsp/ Ci
C1	225.15	225.2	1.930	0.930	0.045	20.66
	225.25					
	225.2					
C2	202.48	202.7	1.737	0.737	0.037	20.14
	202.88					
	202.68					
C3	181.59	181.8	1.558	0.558	0.028	19.8
	181.98					
	181.75					
C4	159.14	159.1	1.363	0.363	0.020	18.47
	159.04					
	159.1					
C5	139.99	139.9	1.199	0.199	0.011	17.65
	139.86					
	139.75					

*t_0=116.965

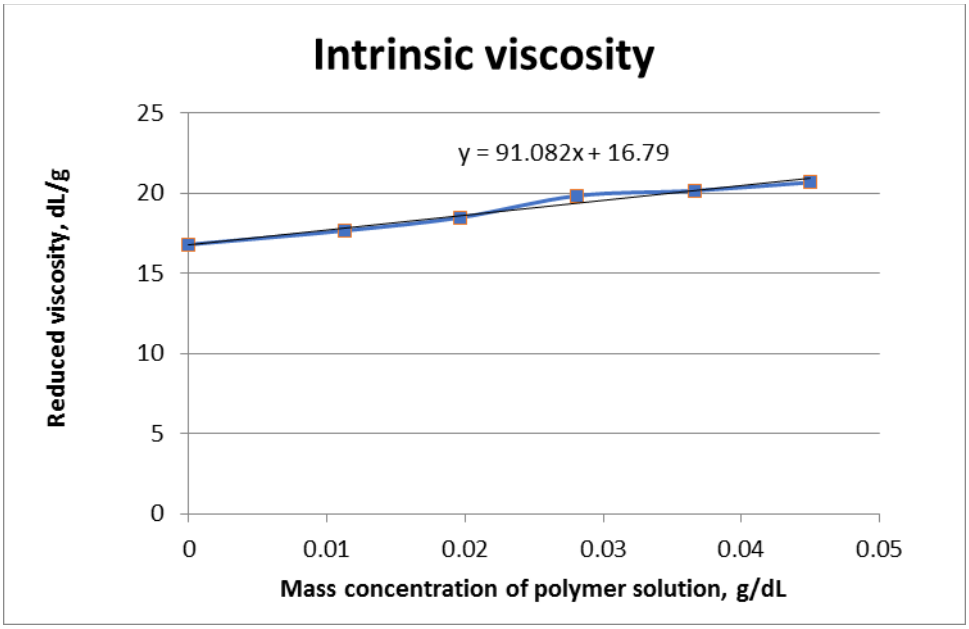

Figure C 2 Intrinsic viscosity of sample FP5115

Table C 5Intrinsic viscosity of sample FP5205

	Polymer drainage time , sec. (t)	Average polymer drainage time , sec. (t avr)	Relative viscosity ηrel=tavr/ t_{0*}	Specific viscosity, ηsp = ηrel -1	Mass concentration of polymer solution, g/dL Ci	Reduced viscosity, dL/g ηsp/ Ci
C1	227.15	227.2	1.947	0.947	0.045	21.03
	227.28					
	227.1					
C2	204.28	204.4	1.752	0.752	0.037	20.54
	204.41					
	204.58					
C3	182.59	182.8	1.566	0.566	0.028	20.13
	182.98					
	182.75					
C4	159.94	160.0	1.371	0.371	0.020	18.85
	159.99					
	159.94					
C5	141.09	141.1	1.209	0.209	0.011	18.56
	141.06					
	141.05					

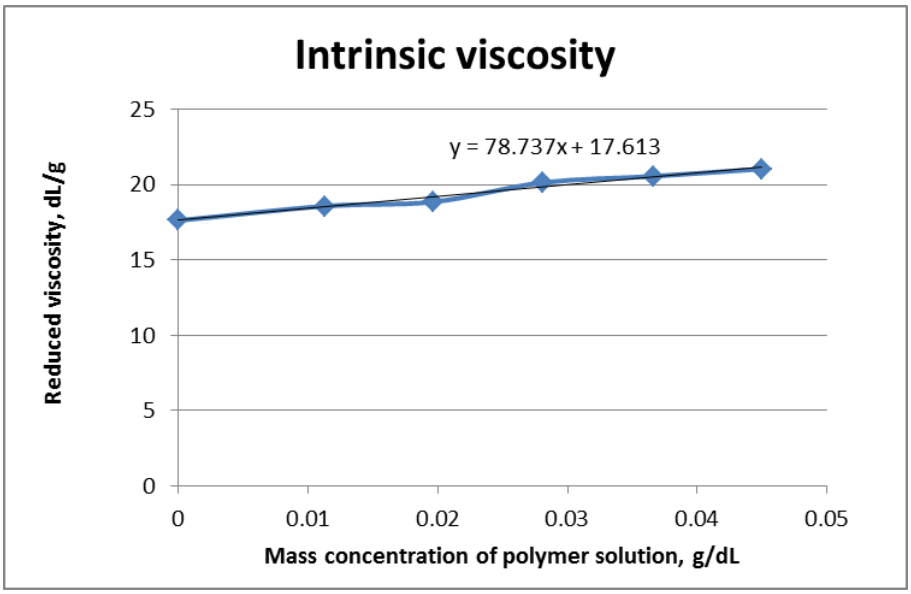

Figure C 3 Intrinsic viscosity of sample FP5205

Appendix D

Appendix D presents the Matlab code for calculation IPV and adsorbtion, and raw data from experiment.

Matlab code

```
%read initial data
A=dlmread('sample2_all.txt');
t=A(:,1);
dp=A(:,2);
res=A(:,3);

%calculating viscosity, polymer concentration and norm.conc

mu=(dp*6894.7573*3.14*((0.089/2)^4))/(8*414*(2/60))*1000; %viscosity
C_pol=((mu-0.7735)/0.0041)/10^6; %polymer conc in g/cc
C_pol_norm=C_pol/0.001513;

%calculating conductivity, tracer concentration and norm.conc

R=res*0.023854; %ohm/m
cond =10./R;%mS/cm

C_tr=(cond-72.062)/(0.7141*1000); %g/cc
C_tr_norm=(C_tr-0.1)/(0.15-0.1);

%calculating PV

PV=t*(2/60)/9.71; %#ofPV

%IPV
t1=A(152:212,1);
pv=t1*(2/60)/9.71; %#ofPV

dp1=A(152:212,2);
mu1=(dp1*6894.7573*3.14*((0.089/2)^4))/(8*414*(2/60))*1000; %viscosity
c_pol=((mu1-0.7735)/0.0041)/10^6; %polymer conc in g/cc
c_pol_norm=c_pol/0.001513;

res1=A(152:212,3);
R1=res1*0.023854; %ohm/m
cond1 =10./R1;
c_tr=(cond1-72.062)/(0.7141*1000);
c_tr_norm=(c_tr-0.1)/(0.15-0.1);

integral_polymer1 = trapz(pv,c_pol_norm);
integral_tracer1 = trapz(pv,c_tr_norm);
ipv=integral_tracer1-integral_polymer1;
IPV=ipv/9.71;
disp(['IPV = ',num2str(IPV) ]);


% Absorption calculation
```

```
t2=A(1:59,1); % PV for absorption calculation
pv1=t2*(2/60)/9.71; %#ofPV
dp2=A(1:59,2); % polymer curve for absorption calculation
mu2=(dp2*6894.7573*3.14*((0.089/2)^4))/(8*414*(2/60))*1000; %viscosity
c_pol1=((mu2-0.7735)/0.0041)/10^6; %polymer conc in g/cc
c_pol_norm1=c_pol1/0.001513;
res2=A(1:59,3); %tracer curve for absorption calculation
R2=res2*0.023854; %ohm/m
cond2 =10./R2;
c_tr1=(cond2-72.062)/(0.7141*1000);
c_tr_norm1=(c_tr1-0.1)/(0.15-0.1);


integral_polymer = trapz(pv1,c_pol_norm1); % area under polymer curve
integral_tracer = trapz(pv1,c_tr_norm1); % area under tracer curve

A=integral_tracer-integral_polymer; % difference in areas

Ads=(A+ipv)*9.71*.001513/106.88;
pol_abs=Ads*106.88;
disp(['Adsorption1 = ',num2str(Ads), ' g/g' ]);
disp(['Polymer absorbed1 = ',num2str(pol_abs), ' g' ]);

figure(1);
figure('Units','centimeters','color','w')
subplot(2,2,1);
plot(PV,C_pol_norm,PV,C_tr_norm)
ylim([0 1])
legend('Cp = polymer production curve','Ct = tracer production curve')
title('concentration vs PV','FontSize',16)
xlabel('Pore Volume','FontSize',14)
ylabel('Normalized Concentration','FontSize',14)
legend('Location','SouthOutside')
subplot(2,2,2);
figure('Units','centimeters','color','w')
plot(pv,c_pol_norm,pv,c_tr_norm)
ylim([0 1])
title('IPV','FontSize',16)
xlabel('Pore Volume','FontSize',14)
ylabel('Normalized Concentration','FontSize',14)
subplot(2,2,3);
figure('Units','centimeters','color','w')
plot(pv1,c_pol_norm1,pv1,c_tr_norm1);
ylim([0 1])
title('Adsorption','FontSize',16)
xlabel('Pore Volume','FontSize',14)
ylabel('Normalized Concentration','FontSize',14)
```

Raw data from experiment

t	Pressure gradient,psi	resistance, ohm
1	2	3
0	-0.009	1.006
60	-0.009	2.910
120	-0.008	2.912
180	-0.008	2.846
240	0.252	2.849
300	0.361	2.800
360	0.515	2.802
420	0.644	2.755
480	0.805	2.757
540	1.006	2.741
600	1.006	2.781
660	1.059	2.773
720	1.115	2.766
780	1.174	2.711
840	1.236	2.654
900	1.301	2.653
960	1.369	2.643
1020	1.139	2.636
1080	1.522	2.572
1140	1.697	2.571
1200	1.974	2.571
1260	2.215	2.569
1320	2.778	2.513
1380	3.015	2.515
1440	3.325	2.516
1500	3.800	2.516
1560	3.772	2.453
1620	4.293	2.452
1680	4.346	2.451
1740	4.590	2.448
1800	5.224	2.447
1860	5.872	2.446
1920	5.692	2.411
1980	6.017	2.412
2040	6.154	2.410
2100	6.378	2.409
2160	5.852	2.401
2220	6.621	2.400
2280	6.161	2.399
2340	6.632	2.398

1	2	3
2400	7.068	2.384
2460	6.516	2.383
2520	7.011	2.383
2580	6.717	2.382
2640	6.619	2.381
2700	6.979	2.380
2760	7.192	2.379
2820	6.713	2.379
2880	7.347	2.377
2940	7.068	2.377
3000	7.740	2.376
3060	7.442	2.376
3120	8.189	2.377
3180	7.987	2.379
3240	8.288	2.380
3300	7.956	2.380
3360	7.773	2.375
3420	8.360	2.375
3480	7.931	2.375
3540	8.064	2.375
3600	8.302	2.361
3660	8.698	2.361
3720	8.398	2.361
3780	8.297	2.361
3840	8.458	2.368
3900	8.146	2.368
3960	8.342	2.369
4020	7.866	2.369
4080	8.475	2.362
4140	8.324	2.363
4200	7.763	2.363
4260	8.428	2.363
4320	7.707	2.363
4380	8.591	2.363
4440	7.955	2.364
4500	8.323	2.364
4560	7.680	2.364
4620	8.126	2.364
4680	8.177	2.365
4740	7.835	2.365
4800	8.867	2.358
4860	7.826	2.359
4920	8.151	2.359
4980	8.033	2.360

1	2	3
5040	7.561	2.361
5100	8.182	2.362
5160	8.198	2.364
5220	7.928	2.365
5280	8.232	2.367
5340	7.956	2.368
5400	7.706	2.355
5460	8.317	2.357
5520	7.655	2.358
5580	8.141	2.360
5640	7.833	2.361
5700	8.372	2.363
5760	9.075	2.364
5820	8.023	2.353
5880	8.265	2.346
5940	8.629	2.345
6000	8.689	2.346
6060	8.853	2.343
6120	9.030	2.340
6180	8.643	2.343
6240	7.834	2.340
6300	8.307	2.340
6360	8.738	2.340
6420	8.263	2.340
6480	8.406	2.340
6540	8.212	2.340
6600	8.088	2.343
6660	8.479	2.341
6720	7.808	2.340
6780	8.964	2.340
6840	8.238	2.344
6900	8.308	2.342
6960	8.393	2.340
7020	8.881	2.345
7080	7.895	2.343
7140	8.121	2.343
7200	8.313	2.345
7260	8.421	2.351
7320	8.391	2.357
7380	8.681	2.353
7440	8.723	2.346
7500	8.212	2.354
7560	7.718	2.359
7620	8.111	2.347

1	2	3
7680	8.329	2.357
7740	7.546	2.352
7800	7.911	2.347
7860	8.106	2.350
7920	8.242	2.346
7980	7.803	2.351
8040	8.373	2.347
8100	8.282	2.340
8160	8.003	2.353
8220	8.307	2.346
8280	8.463	2.346
8340	8.485	2.353
8400	8.337	2.357
8460	8.261	2.353
8520	7.985	2.353
8580	8.140	2.353
8640	8.594	2.353
8700	8.715	2.360
8760	8.401	2.365
8820	8.666	2.367
8880	8.086	2.365
8940	8.692	2.369
9000	8.618	2.371
9060	8.586	2.374
9120	7.969	2.373
9180	8.370	2.378
9240	8.065	2.379
9300	8.258	2.382
9360	8.095	2.385
9420	8.304	2.387
9480	8.217	2.393
9540	7.609	2.394
9600	7.663	2.415
9660	8.027	2.416
9720	7.819	2.415
9780	7.241	2.414
9840	7.220	2.414
9900	7.164	2.412
9960	6.886	2.429
10020	7.170	2.472
10080	7.324	2.486
10140	6.603	2.478
10200	6.912	2.481
10260	6.922	2.500

1	2	3
10320	6.000	2.497
10380	5.734	2.493
10440	6.308	2.491
10500	5.361	2.489
10560	5.746	2.504
10620	5.103	2.523
10680	5.160	2.515
10740	5.142	2.515
10800	5.316	2.514
10860	4.870	2.536
10920	4.892	2.533
10980	3.450	2.536
11040	3.515	2.539
11100	2.742	2.541
11160	3.339	2.544
11220	2.479	2.604
11280	2.191	2.606
11340	1.481	2.608
11400	1.435	2.612
11460	1.177	2.619
11520	1.376	2.626
11580	1.419	2.627
11640	1.420	2.689
11700	0.846	2.692
11760	0.848	2.694
11820	0.816	2.714
11880	1.760	2.749
11940	2.102	2.751
12000	0.872	2.778
12060	1.196	2.804
12120	1.100	2.805
12180	1.865	2.806
12240	1.676	2.805
12300	1.133	2.809
12360	1.466	2.826
12420	0.224	2.858
12480	0.534	2.883
12540	0.086	2.892
12600	0.288	2.895
12660	0.357	2.900